Palaeogeography, Palaeoclimatology, Palaeoecology 497 (2018) 168–185

Contents lists available at ScienceDirect

Palaeogeography, Palaeoclimatology, Palaeoecology

journal homepage: www.elsevier.com/locate/palaeo

Isotope records (C-O-Sr) of late Pliensbachian-early Toarcian environmental perturbations in the westernmost Tethys (Majorca Island, Spain)

Idoia Rosales[a,*], Antonio Barnolas[a], Antonio Goy[b], Ana Sevillano[c], Maider Armendáriz[a], José María López-García[c]

[a] Instituto Geológico y Minero de España (IGME), La Calera 1, 28770, Tres Cantos, Madrid, Spain
[b] Departamento de Paleontología, Facultad de Ciencia Geológicas, Universidad Complutense de Madrid, 28040 Madrid, Spain
[c] Instituto Geológico y Minero de España (IGME), Unidad territorial de Baleares, 07007 Palma de Mallorca, Spain

ARTICLE INFO

Keywords:
Stable isotopes
Strontium isotopes
Sea-level change
Hyperthermal event
Early Jurassic

ABSTRACT

The late Pliensbachian–early Toarcian (Early Jurassic) was a time of major environmental changes that culminated with the Early Toarcian Oceanic Anoxic Event (T-OAE, ca. ~183 Ma). This period is marked by significant disturbances in the carbon cycle and rapid climatic changes. To improve the understanding of the expression of these events in westernmost Tethyan domains, this study provides new belemnite and bulk carbonate C and O stable isotope records of a ~5 Myr upper Pliensbachian to middle Toarcian marine succession of the Balearic Basin (Es Cosconar section, Majorca). Time resolution has been improved by combination of biostratigraphic (ammonoids and brachiopods) and geochronologic ($^{87}Sr/^{86}Sr$) methods. Seawater paleotemperatures derived from $\delta^{18}O$ belemnite records reveal cooler paleotemperatures in the upper part of the *Spinatum* Zone. The uppermost *Spinatum* Zone is characterized by the onset of a warming event that crosses the Pliensbachian-Toarcian boundary, culminating with the warmer temperatures (up to ~10 °C of warming) for the *Serpentinum* Zone of the lower Toarcian. This warming event has been detected contemporaneously in many other European and Tethyan basins and is interpreted to represent generalized raised seawater temperatures linked to the T-OAE. Four significant $\delta^{13}C$ events have been recorded in belemnite and bulk carbonate records. The first is a negative carbon isotope excursion (CIE) around the Pliensbachian-Toarcian boundary, which is best represented in the belemnite record. Soon after, the bulk-carbonate record shows a positive shift in the lower *Tenuicostatum* Zone concomitant with a return to background values in the belemnite record, suggesting strong water stratification or decoupling probably related with export of neritic carbonate to the basin. The third is a negative CIE represented in bulk carbonate across the *Tenuicostatum-Serpentinum* zonal transition, which could be correlated with the negative excursion characterizing the onset of the T-OAE in other sections. The position of this excursion corresponds with a gap in the belemnite record. Finally, in the lower Toarcian, both the bulk carbonate and belemnite carbon isotope records show pronounced positive CIEs in the lower-middle part of the *Serpentinum* Zone. These CIEs testify the impact of the T-OAE in the Balearic basin.

1. Introduction

The Jurassic was a time of major paleoclimatic, paleogeographic and paleoceanographic changes, of which the Early Toarcian Oceanic Anoxic Event (T-OAE; ~183 Ma) is the only event recognized to date that is considered clearly global in its effects (e.g. Hesselbo et al., 2000; Jenkyns, 2010). It coincided with a period of major paleogeographic reorganization (Fig. 1), due to the opening of the Central Atlantic Ocean during the break up of Pangea, the formation of the Karoo-Ferrar large igneous province (LIP) in southern Gondwana (Pálfy and Smith, 2000; Jourdan et al., 2008), and the climax of a second-order eustatic transgression with rapid rise of sea level (Hallam, 1997). The confluence of these events triggered a significant paleoclimatic and paleoenvironmental change that resulted in conditions of oceanic warming and anoxia with widespread deposition of organic-rich shales and a dramatic impact on the marine environment, which led eventually to mass extinctions (Little and Benton, 1995; Hallam and Wignall, 1999; Harries and Little, 1999; Wignall et al., 2005; Dera et al., 2010; Gómez and Goy, 2011; García Joral et al., 2011). This event has been related also to significant perturbations in the global carbon cycle that gave rise to carbon isotopic excursions (CIEs) in all carbon reservoirs (Hesselbo et al., 2000, 2007). The CIEs were accompanied by

* Corresponding author.
E-mail address: i.rosales@igme.es (I. Rosales).

https://doi.org/10.1016/j.palaeo.2018.02.016
Received 25 August 2017; Received in revised form 13 February 2018; Accepted 13 February 2018
Available online 20 February 2018
0031-0182/

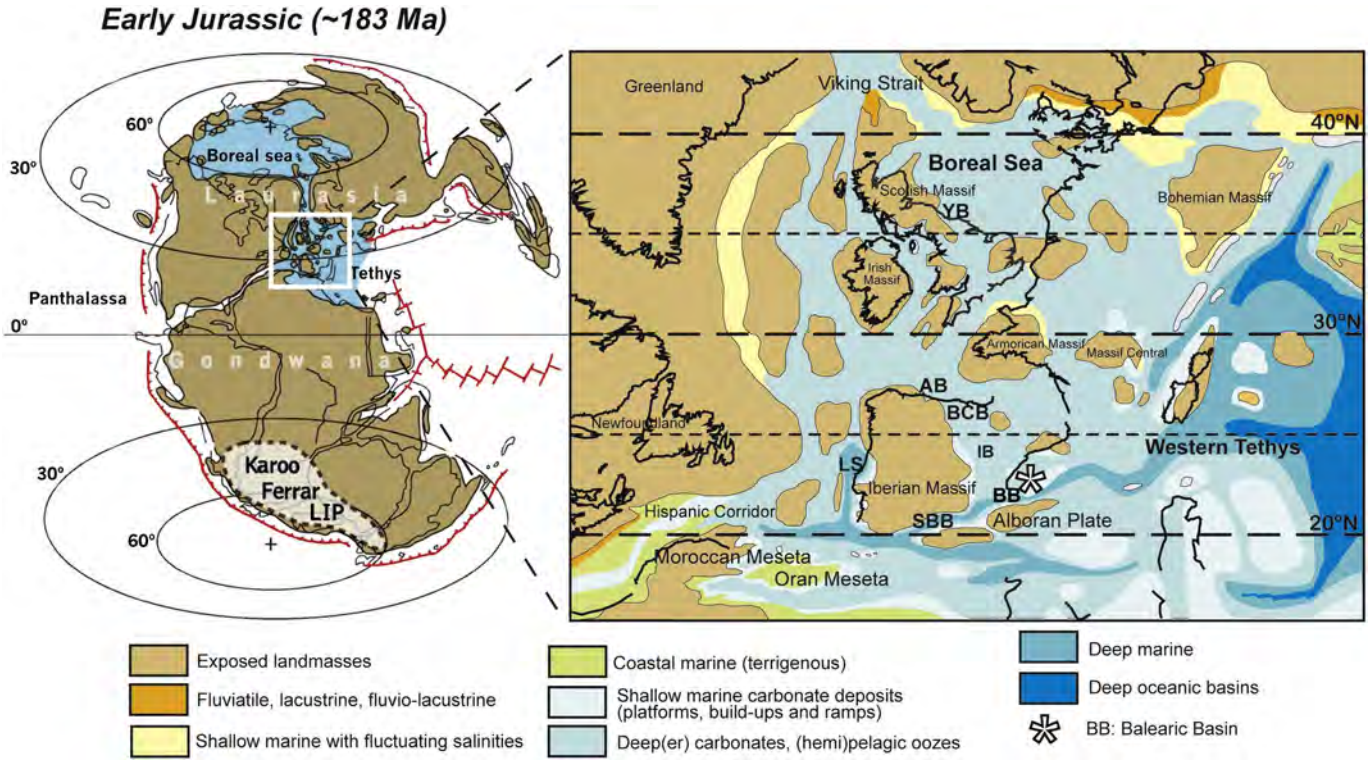

Fig. 1. General Pliensbachian-Toarcian (Early Jurassic) paleogeographical context of the study area at global scale and in the Western Tethyan realm. Modified from Dera et al. (2010) and Dercourt et al. (2000). Cited basins from North to South, YB: Yorkshire Basin, AB: Asturian Basin, BCB: Basque-Cantabrian Basin, IB: Iberian Basin, LS: Lusitanian Basin, BB: Balearic Basin, SBB: Sub-Betic Basin.

minimum Sr-isotope values (Jones et al., 1994; Jenkyns, 2010) and a negative oxygen isotope excursion, triggered presumably by global warming. All these geochemical anomalies have been reproduced in many lower Toarcian sections around the world, despite the regional presence or not of anoxic deposits.

The issue of the T-OAE duration is complicated by different definitions of the T-OAE and of associated CIEs. Most authors use the presence of a negative CIE in marine sediments, recorded during the upper *Tenuicostatum* to lowermost *Falciferum/Serpentinum* zones in both organic and carbonate carbon, as the geochemical expression that defines the T-OAE. These authors give several estimates for the duration of the negative CIE, ranging the most recent publications between 0.6 Myr (Huang and Hesselbo, 2014; Ruebsam et al., 2014) and 0.3 to 0.5 Myr (Boulila and Hinnov, 2017), based on astronomical chronology and cyclostratigraphy. It should be noted, however, that these studies use different definitions for the negative CIE interval. Using the definition of Boulila and Hinnov (2017) and the time scale of Huang and Hesselbo (2014), the CIE may have lasted more that 1.4 Myr. Other studies define the duration of T-OAE as an interval that begins with the negative CIE at the *Tenuicostatum* Zone and follows with a pronounced positive CIE in the middle/upper part of the *Falciferum* Zone (equivalent to the *Serpentinum* or *Levisoni* zones in the Tethyan schemes) (e.g. Hesselbo et al., 2000; Jenkyns et al., 2002). The later is best identifiable in the dataset presented here, like in other records of Spain (Rosales et al., 2004a, 2004b, 2006; Gómez et al., 2016a, 2016b). This T-OAE interval is preceded in some sections by a negative shift during the Pliensbachian-Toarcian transition (Pl-To transition). The interval between the Pl-To transition and the highest carbon isotope values marking the positive CIE has an estimated duration ranging between < 1 Myr (Boulila and Hinnov, 2017) and up to 2.5 Myr (Huang and Hesselbo, 2014).

The mechanisms and the local versus global origin of the negative isotopic excursion at the onset of the T-OAE are still under debate. Although many authors now accept that it was global and synchronous worldwide and that affected to all the carbon reservoirs (Hesselbo et al., 2007; Hermoso et al., 2009, 2012; Littler et al., 2010; Suan et al., 2011), other studies have questioned its global nature because some profiles, especially those based on belemnite calcites, do not seem to record clearly the negative shift (van de Schootbrugge et al., 2005a; Rosales et al., 2006; Gómez et al., 2008; Metodiev and Koleva-Rekalova, 2008).

Oxygen isotope data indicate that the T-OAE was also a thermal event characterized by a global rapid rise in seawater paleotemperatures of about 5–7 °C in average (e.g. Bailey et al., 2003; Rosales et al., 2004a; Gómez and Goy, 2011; Korte et al., 2015; Gómez et al., 2016a). This temperature maximum succeeded a cooling phase (late Pliensbachian Cooling Event), evidenced by a shift to more positive $\delta^{18}O$ values, which appears to have occurred also synchronously in many basins during the late Pliensbachian *Spinatum* Zone (Rosales et al., 2001, 2004a, 2004b, 2006; Bailey et al., 2003; Gómez et al., 2008; Suan et al., 2010; Dera et al., 2011; Korte et al., 2015; Gómez et al., 2016a). These cooling and warming episodes may correlate respectively with second order regressive and transgressive sea-level phases (e.g. Quesada et al., 2005; Rosales et al., 2006; Suan et al., 2010), suggesting probably glacio-eustatic or supraregional tectonic controls on the isotopic and sedimentary records around the Pliensbachian–Toarcian transition (Korte et al., 2015).

An amount of the data supporting these interpretations come from epicontinental basins of Boreal, sub-Boreal or sub-Mediterranean seas (Fig. 1), but these epicontinental records may reflect strong regional overprint upon the C and O isotope records, because these basins likely became intermittently salinity stratified and developed strong haloclines and thermoclines (e.g. Podlaha et al., 1998; Rosales et al., 2004b; Harazim et al., 2012). Thus, more archives from other regions representative of different water masses are needed. In order to improve the understanding of the expression of these events in other paleogeographic regions, this study aims to reconstruct the long-term evolution of paleoclimatic changes and major perturbations of the geochemical cycles during the late Pliensbachian–middle Toarcian interval (~5 Myr)

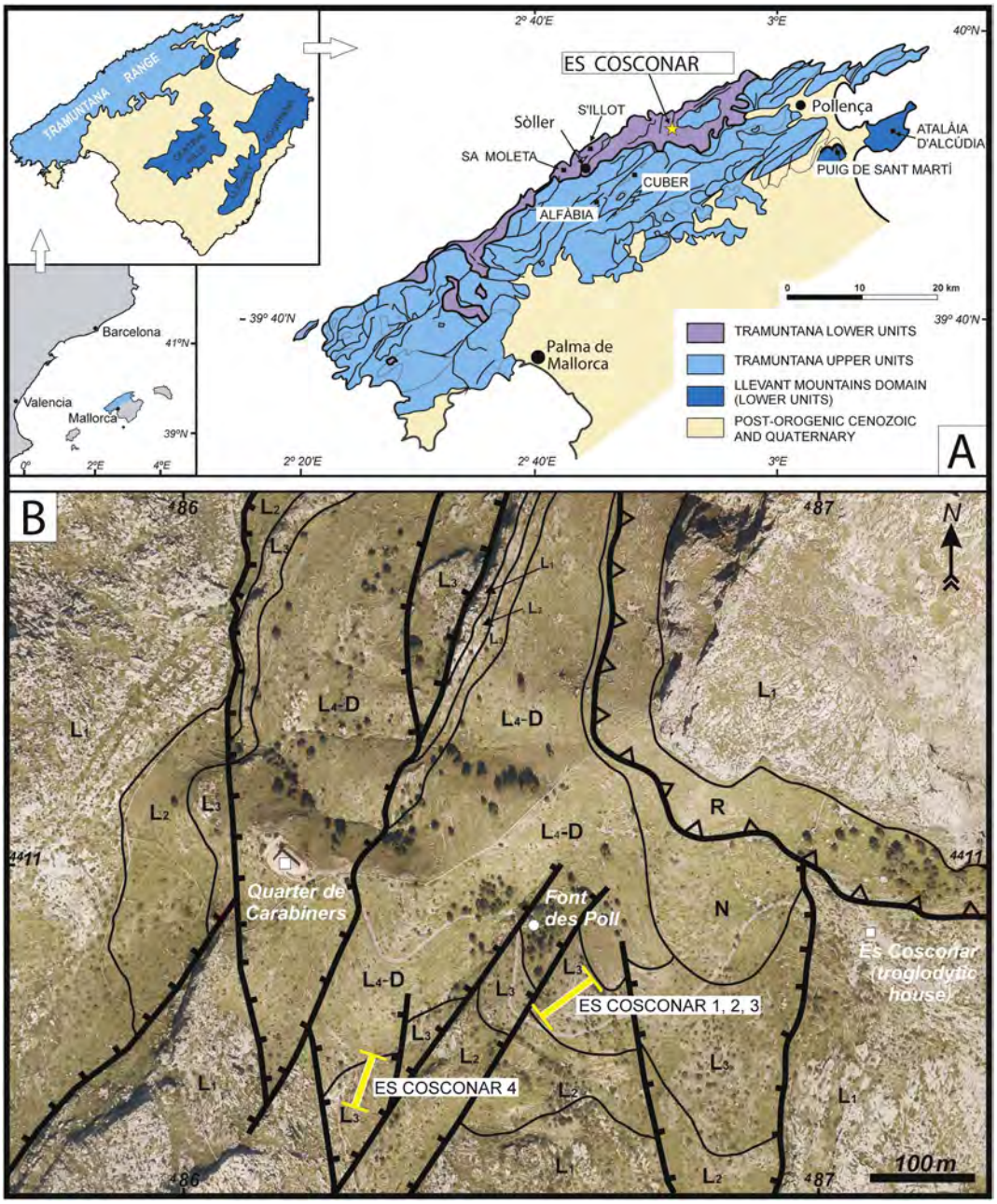

Fig. 2. A. Structural sketch of the Tramuntana range in the Majorca island with location of Es Cosconar and other sites referred in this work (modified from Gelabert, 1998). B. Geological map of the Es Cosconar outcrop, in the Tramuntana range of Majorca, showing the location of the four logged and sampled sections (Es Cosconar 1, 2, 3 and 4). R: Rhaetian red shales and dolomites; L1: Hettangian and Sinemurian shallow platform carbonates; L2: Lower Pliensbachian marls (Sa Moleta Mb) and siliciclastic sandstones-conglomerates (Es Racó Mb); L3: crinoidal limestones (Es Cosconar Fm); L4-D: marls and marly limestones (Gorg Blau and Cuber Fms); N: Upper Oligocene- Lower Neogene conglomerates. Numbers in the margin of the picture are UTM coordinates. (For interpretation of the references to colour in this figure legend, the reader is referred to the web version of this article.)

recorded in carbonate geochemistry from the Balearic domain, which is representative of a paleogeographic position in the westernmost Tethys (Fig. 1). The study provides new chemostratigraphic ($\delta^{13}C$, $\delta^{18}O$, $^{87}Sr/^{86}Sr$) records of a relatively expanded section of the Majorca island (Es Cosconar section; Fig. 2). This is the only stratigraphic profile of the Balearic Basin that provides a continuous and relatively complete record for this time interval, because in other sections of the Balearic domain most of the Toarcian succession is condensed into a ferruginous hardground (Prescott, 1988; Álvaro et al., 1989). Thus, this section represents the only stratigraphic frame for such a study. The records have been time-constrained against a new (revised) biostratigraphy obtained from ammonites and brachiopods, and a new Sr-isotope ($^{87}Sr/^{86}Sr$) chronostratigraphy that improves the chronostratigraphic framework based on the biostratigraphy.

2. Geological setting

The Balearic archipelago, in the western Mediterranean Sea, constitutes the northeast extension of the Rifean-Betic alpine orogenic arc (Azañon et al., 2002). Majorca is the biggest island of this archipelago, which is constructed mainly by folded and thrusted Mesozoic–Lower Cenozoic rocks arranged into three NE-SW oriented mountain belts (Tramuntana range, Central hills and Llevant mountains; Fig. 2A). These mountains are partially surrounded by low land plains of younger, post-orogenic unconformably sedimentary rocks.

The existence in the Balearic Basin of different structural domains

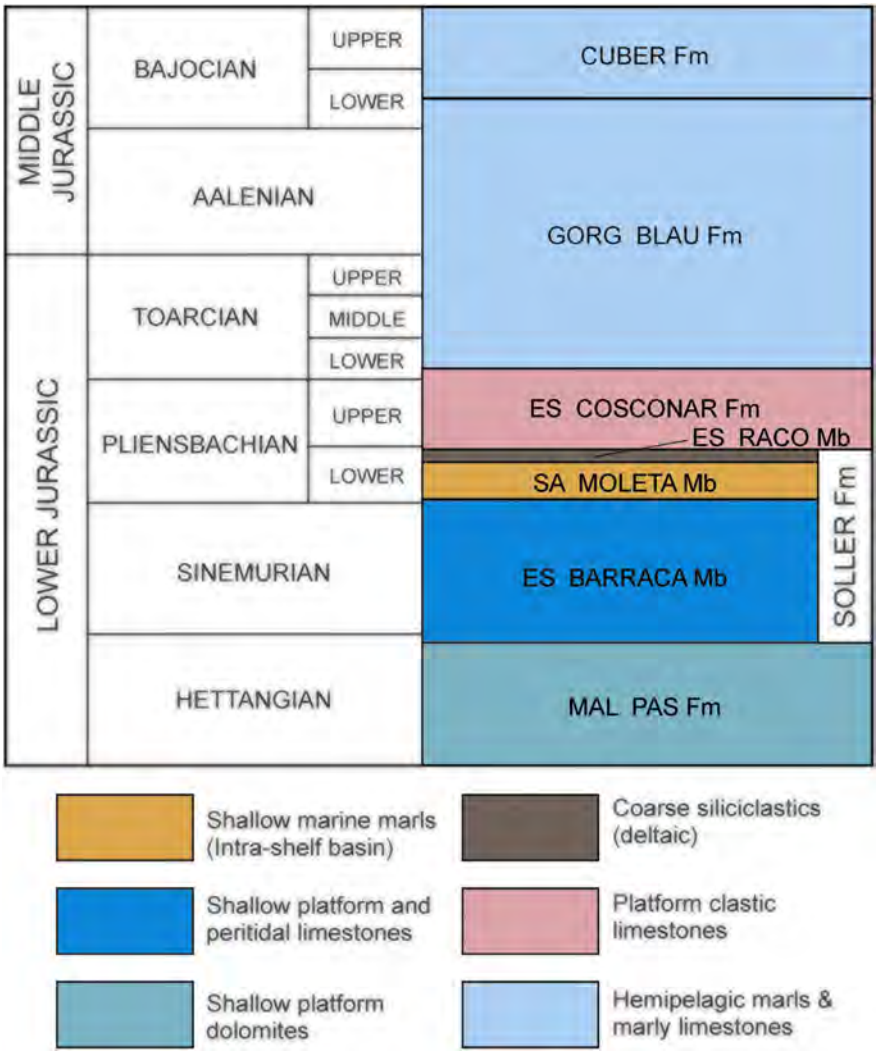

Fig. 3. Lithostratigraphic chart of the Jurassic in the Es Cosconar area in the Lower Units of the Tramuntana range. Modified from Álvaro et al. (1989).

with different Jurassic stratigraphies has been interpreted as a consequence of the Alpine tectonic inversion of an ancient Jurassic rifted margin (Barnolas and Simó, 1984), related to the opening of the Central Atlantic Ocean and the extensional transference of the Tethys Ocean in its westward progression (Dewey et al., 1973; Dercourt et al., 2000). The Balearic Basin (BB in Fig. 1), located in the Iberian margin, was placed in a point that connected the Hispanic Corridor, the Boreal Sea and the Western Tethys (Fig. 1), recording a progressive influence of Tethyan waters during the Jurassic. The Jurassic stratigraphy of Majorca was established by Álvaro et al. (1989), and it is summarized in Fig. 3 for the Es Cosconar area. The analyzed interval belongs to the upper Pliensbachian Es Cosconar Formation, made of platform limestones, and the lower part of the hemipelagic Toarcian–Aalenian Gorg Blau Formation (Fig. 3).

3. Materials and methods

The studied Es Cosconar section of the Majorca island is located in the Tramuntana range domain, about 14 km to the northeast of the Soller town (Majorca), geographic coordinates 39°50′41.49″N, 2°50′32.48″E (Fig. 2B). It is one of the most complete and fossiliferous Pliensbachian-Toarcian sections of the Majorca island. The section has been described and studied previously by Fallot (1922), Colom (1942) and Álvaro et al. (1989). The section is exposed in the slopes of a forest track that goes from the troglodytic houses of Es Cosconar to an old abandoned border guard station (Quarter de Carabiners; Fig. 2B), now rebuilt. During the field survey, the section was stratigraphically logged bed by bed along four profiles (Cos1 to Cos4, Fig. 2B), and all the beds numbered consecutively in the field from bed 1 to bed 262. The four sections have been merged into a composite section of the entire upper Pliensbachian–middle Toarcian succession. Sections Cos2 and Cos3 are continous and placed only few tens of meters apart, and for simplifying, both sections have been merged in one single section named Cos2/3 (Fig. 4). Physical correlation between Cos1 and Cos2/3 sections was accomplished by the lateral field continuity of individual beds between the two sections (e.g. bed 24 of Cos1 corresponds to bed 100 of Cos2/3; Fig. 4). The base of section Cos4 (Fig. 4), ~300 m to the southwest of the base of Cos1 (Fig. 2B), is separated from the other outcrop for a fault, and the stratigraphic correlation between the two outcrops was based on biostratigraphic data and the correlation of a lithologically distinctive horizon of yellowish-tan, bioturbated sandy calcarenites with abundant gastropods that is recognized in the two outcrops at the base of the *Tenuicostatum* Zone (marked in yellow in Fig. 4). Rock samples, belemnites, ammonites and brachiopods were stratigraphically collected from these sections for chemostratigraphic and biostratigraphic determinations at zonal and subzonal level.

The analyses for the chemostratigraphy were performed on both belemnite and bulk carbonate samples. Belemnites were collected only from the Cos1-2/3 sections. Belemnites were microsampled under a binocular microscope with a dental drill for carbon, oxygen and

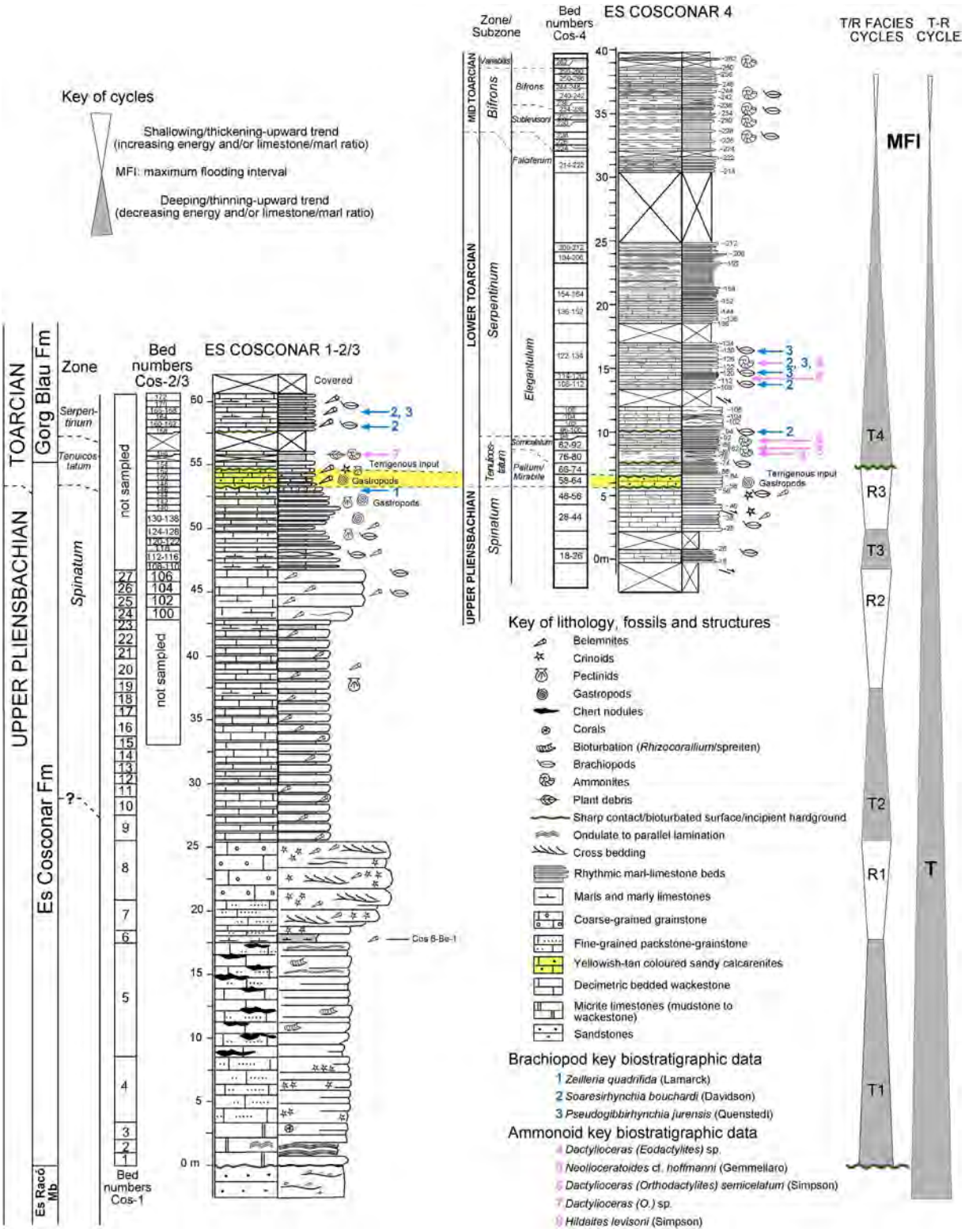

Fig. 4. Lithology, biochronozones and bed numbers of sampled levels for the four logged sections at the Es Cosconar outcrop, with indication of correlation beds between the two principal outcrops and key biostratigraphic ammonite and brachiopod data. Correlation is based on the biostratigraphic information, the stratigraphic position of a marker interval of silty-sandy yellowish-tan calcarenites with gastropods and a disconformity surface (bioturbated surface) at the base of the *Tenuicostatum* Zone. (For interpretation of the references to colour in this figure legend, the reader is referred to the web version of this article.)

strontium isotope analyses, avoiding apical line and microfractures. The common incomplete preservation of the belemnite rostra does not allow confident assignment of all specimens to a particular genus, with exception of some complete rostra attributable to *Passaloteuthis*, *Hastites* and *Acrocoelites*. The low degree of diagenetic alteration of the belemnite samples was confirmed by measuring the Mn, Sr, Fe, Mg, Na and Ca elemental contents of subsamples, using an inductively coupled plasma-atomic emission spectrometer (ICP-AES model Varian Vista MPX) of the laboratories of the Instituto Geológico y Minero de España (IGME) in Madrid. Detection limits for Ca, Fe, Mg, Mn, Na and Sr are

1000, 200, 100, 50, 100 and 10 ppm, respectively. A total of 120 belemnite calcite microsamples were analyzed for their carbon and oxygen isotope composition. For the bulk-carbonate isotopic analysis, 132 samples were collected in the field at regular intervals of about 1 m. In the lab, the bulk-rock carbonate material was carefully extracted using a microscope-mounted dental drill avoiding observable fossils, fractures, stylolites and cements.

Carbon and oxygen stable isotope data ($\delta^{13}C$ and $\delta^{18}O$) were collected from the CO_2 gas liberated by the carbonate powders, after reacting online with 103% H_3PO_4 at 25 °C, using the standard digestion method described in McCrea (1950). The analyses were performed on a SIRA-II mass spectrometer at the Servicio General de Análisis de Isótopos Estables of the Universidad de Salamanca (Spain). Carbon- and oxygen-isotope ratios are expressed in the usual δ-notation in parts permil (‰) relative to the Vienna Pee Dee Belemnite (V-PDB) standard. Samples were calibrated against the internal carbonate standard EEZ-1 (values of 2.30‰ and −4.69‰ for $\delta^{13}C$ and $\delta^{18}O$ respectively). The analytical error was 0.09‰ for the $\delta^{13}C$ and 0.17‰ for the $\delta^{18}O$ ($n = 21$).

For strontium isotope analysis, 24 belemnite subsamples were selected mainly from the upper Pliensbachian and Pliensbachian-Toarcian transition, for improving the chronostratigraphic resolution of this ammonites-poor part of the succession. The Sr isotopic composition was determined with a TIMS-Phoenix mass spectrometer at the Laboratorio de Geocronología y Geoquímica Isotópica of the Universidad Complutense de Madrid (Spain). Strontium was separated by standard methods of dissolution, column chromatography and evaporation to dryness. For the chromatographic separation of the Sr a SrResinTM extraction resin was used. The Sr was then recovered with 0.05 M HNO_3. The fraction that contains the Sr concentrate was dried and placed in Re filaments along with 1 μl of 1 M H_3PO_4 and 2 μl of 2 M Ta_2O_5 for the TIMS spectrometer. All $^{87}Sr/^{86}Sr$ data were corrected for possible ^{87}Rb interferences and were normalized respect to a value of $^{86}Sr/^{88}Sr = 0.1194$. During the period of analysis, the NBS-987 standard was introduced several times, giving an average $^{87}Sr/^{86}Sr$ value of 0.710246 ± 0.000012 (2σ, $n = 7$). These values were used to correct a possible deviation referred to the standard, using as reference a mean $^{87}Sr/^{86}Sr$ value of the standard along the life of the laboratory of 0.710248 ± 0.000005 (2σ, $n = 728$). The analytical error of the $^{87}Sr/^{86}Sr$ ratios was 0.01% (2σ).

4. Results

4.1. Es Cosconar section stratigraphy

4.1.1. Lithological description

The logged upper Pliensbachian to middle Toarcian (*Bifrons* Zone) succession in the Es Cosconar section exhibits ca. 87 m of limestones and marls. The basal *datum* of the section is located on top of cross-bedded pebbly sandstones of the Es Racó Member of the Soller Formation (Fig. 3), which is interpreted to represent a regressive unit of delta sedimentation at the end of the Carixian (Álvaro et al., 1989). On top of these siliciclastics, the upper Pliensbachian succession (Es Cosconar Formation) starts sharply with ca. 2 m of micritic limestone with undulating and parallel cryptoalgal lamination and fenestral porosity (peritidal), followed by ca. 11.5 m of wackestone and fine-grained, laminated crinoidal packstone-grainstone organized in decimetric to metric tabular beds. This part of the succession presents solitary corals, spreiten burrows (rhizocorallid) and abundant chert nodules. It culminates with a centimetric bed of marls with belemnites (bed number 6 in Fig. 4). Above this bed, belemnites are widespread throughout the succession. It follows with ca. 10 m of high-energy, cross-bedded coarse grainstones with abundant debris of crinoids and belemnites (bed numbers 7 and 8, Fig. 4). The rest of the succession up to bed 27 in Cos1, equivalent to bed 106 in Cos2/3 (Fig. 4), consists of a package of ca. 18 m of tabular to nodular, decimetric-bedded wackestones to packstones with thin centimetric (up to 5 cm) marly interbeds. Beds on this package display a general coarsening- and thickening-upward trend up to bed 27/106 (Fig. 4), and are rich in belemnites, brachiopods and pectinid bivalves. Above bed 27/106, the marl/limestone ratio increases and the rest of the Pliensbachian succession (ca. 6.5 m) is made of an alternation of centimetric to decimetric beds of limestones and marls with brachiopods, belemnites and pectinids. Toward the upper part, the last 2 m become brownish and bioclastic, with abundant bioturbation and small planispiral gastropods. The Pliensbachian-Toarcian transition is placed tentatively at or near a bioturbated firmground surface on bed Cos2/3-146 (Fig. 4). This bioturbated firmground surface can be correlated between Cos2/3 and Cos4 sections. Above this surface the next ca. 2 m (in Cos2/3) to 1.5 m (in Cos4) of the succession are constituted by yellowish-tan, terrigenous-rich, silty-sandy bioclastic and bioturbated nodular limestones rich in small gastropods, along with crinoids, belemnites, pectinids and brachiopods, which can be correlated also between Cos2/3 and Cos4 sections (yellow interval in Fig. 4). The top of this interval is a bioturbated, transgressive surface. The brachiopod fauna collected in this interval indicates already an early Toarcian age (see next subchapter). The rest of the Toarcian succession (Gorg Blau Formation) is made of a hemipelagic rhythmic alternation of marl and marly limestone rich in ammonites and brachiopods, with a general increase in the marl/limestone ratio upward.

4.1.2. Lower and middle Toarcian ammonoid and brachiopod biostratigraphy

The “Cosconá (Lluch) site” and its ammonoid and brachiopod associations were first studied in the end of the 19th century and beginning of the 20th century by Nolan (1895) and Fallot (1922, 1932). Later, Colom (1942) collected a large number of fossils of these groups from the Lower Jurassic outcrops of the Es Cosconar site. In general, the presence in the Majorca island of ammonoids, which would enable to establish a fine biochronostratigraphy of the upper Pliensbachian to middle Toarcian, is scarce, except for a ferruginous layer (hardground) where the majority of the fossils found are reelaborated. In the Tramuntana range, this layer shows a record of taxa of the middle Toarcian. Brachiopods of the lower and middle Toarcian are also relatively scarce in the Tramuntana range and very rare in the Llevant mountains. Only exceptionally they are found from some few outcrops of relatively expanded sections such as those located in Es Cosconar and S'Illot (Fig. 2A).

After 75 years without any other biostratigraphic study in the area, the Es Cosconar section has been sampled again in detail in this study. This has allowed to recognize which are the main ammonoid and brachiopod associations recorded, which genera and species disappeared during the early Toarcian marine extinction bioevent reported by various authors (Little and Benton, 1995; Goy et al., 1998; Harries and Little, 1999; Gahr, 2005; Gómez et al., 2008; García Joral and Goy, 2009; García Joral et al., 2011; Gómez and Goy, 2011; Comas-Rengifo et al., 2015, among others), and how these groups recovered after the crisis, for the study area.

The ammonoids and brachiopods collected in this study from the Es Cosconar section correspond to the interval comprised between the upper Pliensbachian (*Spinatum* Zone, *Hawskerense* Subzone) and the middle Toarcian (*Variabilis* Zone, *Variabilis* Subzone). Due to the absence of upper Pliensbachian ammonoids, the boundary between the Pliensbachian (*Spinatum* Zone) and the Toarcian (*Tenuicostatum* Zone) cannot be precisely located. However, the existence of brachiopods of the family Zeilleridae allows making some precisions. In Cos2/3, *Zeilleria quadrifida* (Lamarck) has been collected from bed 146 (or a bed a little more younger). This species characterizes the upper Pliensbachian (*Spinatum* Zone, *Hawskerense* Subzone) (Alméras and Fauré, 2000). Slightly above (beds 148 to 154), *Zeilleria* aff. *scalprata* (Quenstedt) and *Zeilleria subovalis* Roemer (cited in the Languedocian Pyrénées in the *Tenuicostatum* Zone) have been collected. In Cos4, *Zeilleria* aff. *scalprata* (Quenstedt) has been collected from bed 64 and

bed 74, a species typical from the uppermost Pliensbachian in the Ibero-Pyrenean domain (Alméras and Fauré, 2000), but that has been cited by Delance (1969) in the lower Toarcian (*Tenuicostatum* Zone) of Tartareu (Lleida, Spain). On the other hand, Alméras and Fauré (2000) cite this species in the upper Pliensbachian (*Spinatum* Zone, *Hawskerense* Subzone) of the eastern Pyrénées (Alto Ampurdán and Pedraforca areas), and in the lower Toarcian (*Tenuicostatum* Zone, *Paltum* Subzone) of the central French Pyrénées and southern Spanish Pyrénées. Therefore, in the Es Cosconar section, the most probably is that the Pliensbachian-Toarcian boundary is located close to the top but still within the brownish bioclastic limestones of the uppermost part of the Es Cosconar Formation (Fig. 4).

Regarding the Toarcian portion of the section, both ammonites and brachiopods were collected. At the base of the Toarcian the ammonoids are rare and had not been cited previously in sedimentary successions of the *Tenuicostatum* Zone of Majorca. In this study, in the Cos4 section, it has been possible to characterize the *Paltum/Mirabile* Subzone by the presence of *Dactylioceras* (*Eodactylites*) sp. (bed 80) followed by *Neolioceratoides* cf. *hoffmanni* (Gemmellaro) (bed 82), as well as the *Semicelatum* Subzone by the presence of *Dactylioceras* (*Orthodactylites*) *semicelatum* (Simpson) (bed 90), along with other badly preserved *Dactylioceras* (*Orthodactylites*) sp. Ammonoids are notably more frequent in the *Serpentinum* Zone of the lower Toarcian, but even more in the *Bifrons* Zone of the middle Toarcian, from which some species were already documented in the work of Colom (1942). The *Serpentinum* Zone has been possible to be subdivided also, and has been possible to characterize the *Elegantulum* Subzone by the presence of *Hildaites levisoni* (Simpson) in its base (bed 124), and the *Falciferum* Subzone by the presence *Dactylioceras* (*Dactylioceras*) sp. and *Orthildaites* cf. *douvillei* (Haug) in its uppermost part, although the boundary between both subzones remains imprecise (Fig. 4). In the *Bifrons* Zone the succession of species of Hildoceratidae is rather complete and allows to characterize the *Sublevisoni* Subzone by the record of *Hildoceras sublevisoni* Fucini - *Hildoceras lusitanicum* Meister (beds 231–235), and the *Bifrons* Subzone from the record of *Hildoceras apertum* Gabilly - *Hildoceras bifrons* (Bruguière) - *Hildoceras semipolitum* Buckman (beds 238–262). The base of the *Variabilis* Zone has been characterized by the presence of *Haugia* sp. of the group of *Haugia variabilis* (d'Orbigny) (bed 262). This species is associated to *Hildoceras semipolitum* Buckman, which is abundant in the upper part of the *Bifrons* Subzone and that in a large area of the Submediterranean province (Page, 2003) persisted after the lower limit of the *Variabilis* Zone (Goy et al., 1988; Elmi et al., 1989, 1997; Bécaud, 2006; Gómez et al., 2008).

In addition to ammonites, a large number of brachiopods have been identified also in the Toarcian portion of the succession. They can be grouped into the four brachiopod assemblages described by Goy et al. (1998) and García Joral and Goy (2000), with their most significant elements figured in García Joral et al. (2011). In Es Cosconar, species of the assemblage 1 (with taxa typical of the upper Pliensbachian that can remain residually at the base of the Toarcian) such as *Liospiriferina* aff. *nicklesi* (Corroy) (beds 84–92 of Cos4), *Zeilleria quadrifida* (Lamarck) (bed 146 of Cos2/3) and *Zeilleria* aff. *scalprata* (Quenstedt) (beds 64 and 74 of Cos4 and beds 147–154 of Cos2/3), and species of the assemblage 2 (taxa almost exclusive of the *Tenuicostatum* Zone) such as *Quadratyrhynchia attenuata* (Dubar) (marls above bed 74 of Cos4) and *Zeilleria subovalis* Roemer (beds 147–154 of Cos2/3), have been recorded. The assemblage 3 (which includes only one genus, *Soaresirhynchia*, and that is recorded shortly after the early Toarcian extinction event, García Joral et al., 2011) is represented mainly by *Soaresirhynchia bouchardi* (Davidson) and *Soaresirhynchia rustica* (Dubar) (from bed 94 of the Cos4 section and bed 160 of Cos2/3). These species are occasionally associated to *Pseudogibbirhynchia jurensis* (Quenstedt) at the base of the *Serpentinum* Zone (García Joral and Goy, 2000; Alméras and Fauré, 2000). Finally, the assemblage 4 appears in the *Serpentinum* Zone and extends into the *Bifrons* Zone of the middle Toarcian. It is dominated by species of the genera *Telothyris* (from bed 126 of Cos4) and *Homoeorhynchia* (from bed 110 of Cos4) and corresponds to the so-called "Spanish bioprovince of brachiopods" (García Joral et al., 2011). Toward the uppermost part of the *Bifrons* Zone the biodiversity of brachiopods decreases in the whole Submediterranean province, and in Es Cosconar only *Telothyris* cf. *depressa* (Dubar) and *Choffatirhynchia* cf. *turolensis* García Joral and Goy have been recorded.

Lastly, both the ammonoid and brachiopod associations obtained from Es Cosconar are closer to those recognized from the Submediterranean province (S of England, NW Europe, N of Iberia) than those known from the Mediterranean province (Alps, Apennines, S of Iberia).

4.2. Trace elements and belemnite preservation

Apparently well-preserved (translucent) belemnites collected from the Es Cosconar section have been investigated for their Ca, Na, Mg, Fe, Mn and Sr elemental composition. The aim was to screen the samples for the degree of diagenetic alteration using trace element composition and grade of covariation between elemental and isotopic data. The results of the elemental analyses are given in Supplementary Information in the online version (Table S1). Except for one sample, all the investigated belemnite calcites displayed Fe contents below detection limits (< 200 ppm). The only exception displayed a Fe concentration of 273 ppm (see Supplementary Information, Table S1). This is, however, near or within the cut-off values considered elsewhere for pristine, well-preserved belemnites and biogenic calcites (e.g. Rosales et al., 2001; Wierzbowski and Joachimski, 2007; Armendáriz et al., 2008, 2012; Alberti et al., 2012; Benito and Reolid, 2012). The Mn contents of all the analyzed samples are also below detection limits (< 50 ppm). These very low (undetected) Fe and Mn concentrations verify the good chemical preservation of all belemnite calcites used in this study. The Sr concentrations, which vary between 807 and 1679 ppm, and the Sr/Ca ratios are also above the established threshold for well-preserved belemnites not significantly affected by diagenesis (e.g. Wierzbowski, 2004).

Element/Ca ratios of these well-preserved belemnites vary between 7 and 17 mmol/mol for Mg/Ca and between 1 and 2 mmol/mol for Sr/Ca (Fig. 5), with a rough trend toward maximum values around beds Cos1–8 to −12. There is an extensive discussion in literature to establish whether or not the Element/Ca composition of belemnites retains a temperature-dependent signal, with, in general, high Mg/Ca and Sr/Ca ratios being presumably associated to warmer temperatures (e.g. Rosales et al., 2004a; McArthur et al., 2007; Dutton et al., 2007; Nunn and Price, 2010; Armendáriz et al., 2012, 2013; Li et al., 2012; Ullmann et al., 2015; Price et al., 2016). In this study, cross-plots of Mg/Ca and Sr/Ca ratios versus O-isotope composition show a very low, or non-covariance, between these parameters ($r = -0.18$, $p = 0.05$, $n = 120$; and $r = -0.02$, $p > 0.05$, n = 120 respectively, Fig. 5). The lack of correlation might be an artefact of lumping different belemnite species or may argue against a temperature dependence of the Mg/Ca and Sr/Ca composition of belemnites from this region, contrary to the findings of some previous Pliensbachian-Toarcian belemnite studies from northernmore regions (e.g. Bailey et al., 2003; Rosales et al., 2004a; Armendáriz et al., 2013; Price et al., 2016) but in agreement with others (Ullmann et al., 2015). This suggests that the Element/Ca ratios of these belemnites could have been controlled by other factors such as ontogenetic biofractionation during biomineralization (Li et al., 2012; Benito and Reolid, 2012), crystal morphology or calcification rates (Ullmann et al., 2015) rather than temperature.

4.3. Sr-isotope chronostratigraphy and age calibration

Owing to the long residence time of the Sr in the oceans, the Sr-isotope chronostratigraphy is based on the principle that the $^{87}Sr/^{86}Sr$ composition of the oceans is homogeneous at a given geological time, and that the oceanic Sr-isotopic composition is accurately recorded in

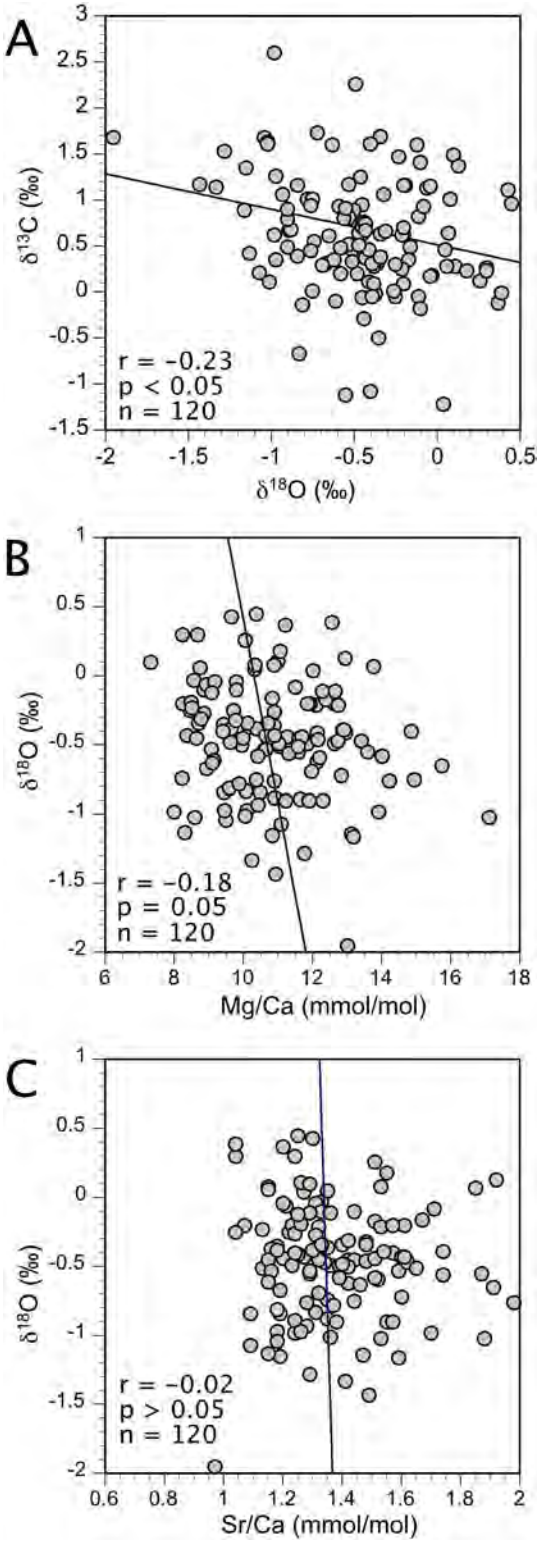

Fig. 5. Scatter plots of geochemical data derived from the studied belemnite calcites showing poor degree of covariance. A. $\delta^{13}C$ versus $\delta^{18}O$. B. $\delta^{18}O$ versus Mg/Ca ratios. C. $\delta^{18}O$ versus Sr/Ca ratios.

calcites precipitated from marine waters (Jones et al., 1994; McArthur, 1994), in this case biogenic belemnite calcites. Therefore, it is assumed that the Lower Jurassic $^{87}Sr/^{86}Sr$ record from well-preserved belemnite calcites from Majorca represents a global signal.

The age-calibration of the Es Cosconar section is principally supported by ammonites and brachiopods (updated in this study), which are widespread in the Toarcian, but scarce for the Pliensbachian. Therefore, the age-resolution of the ammonites-poor interval of the succession has been calibrated with the use of Sr-isotopes. Fig. 6 represents the Sr-isotope record from selected belemnite calcites of Majorca (Es Cosconar section) plotted with projection of the data of McArthur et al. (2000) for the *Margaritatus–Falciferum* (equivalent to *Serpentinum*) zonal interval. The obtained values (see Supplementary Information, Table S2) are coherent with those reported in McArthur et al. (2000). The data show a general decrease from a highest value obtained from bed Cos1–6 to lowest values around bed Cos2/3–144 (Fig. 6). From bed Cos2/3–148 upwards the values show an inflection toward slighlty higher values (Fig. 6). This inflection is a feature that characterizes the Pliensbachian-Toarcian transition (Jones et al., 1994; McArthur et al., 2000; Jenkyns et al., 2002). Therefore, the Sr-isotope chronostratigraphy confirms the location of the Pliensbachian-Toarcian boundary above bed Cos2/3–144, probably around beds Cos2/3–146 to Cos2/3–148 (Fig. 6).

The absolute Sr-isotope values obtained for beds Cos1–6 to −9 (0.707154 to 0.707116) are coherent with the numerical values reported for the upper part of the *Margaritatus* Zone (*Gibbosus* Subzone) (McArthur et al., 2000). The value obtained for bed Cos1–10 (0.707125) is almost the same of that reported by McArthur et al. (2000) for the base of the *Spinatum* Zone (base of *Apyrenum* Subzone, ~184.81 Ma). According to these values the *Margaritatus-Spinatum* zonal boundary has been placed around bed Cos1–10 (Fig. 6). Then, the *Spinatum* Zone comprises the interval between beds Cos1–10 to Cos2/3–146.

4.4. Carbon and oxygen isotope records

All the carbonate carbon and oxygen isotope data obtained from belemnites and bulk carbonate are reported in the Supplementary Information (Table S1 and Table S3) as supporting data.

4.4.1. Bulk carbonate carbon and oxygen isotopes

The studied sections of Es Cosconar allow to produce bulk carbonate (micrite) $\delta^{13}C$ isotope records that span from the late Pliensbachian *Margaritatus* Zone to the middle Toarcian *Bifrons* Zone (Figs. 7 and 8). The $\delta^{13}C_{bulk\text{-}carb}$ values range between −2.9‰ and +2.5‰, displaying a spread of about 5.4‰ (see this in Supplementary Information, Table S3). The temporal record starts with lowest values of ca. –2 to −2.9‰ in the lower *Margaritatus* Zone (not represented in Fig. 7) exhibiting a rapid increase toward higher values above 0‰ (mean 0.6‰) from the upper *Margaritatus* Zone (bed Cos1–6) upwards (see Supplementary Information, Table S3). The highest values (up to +2.5‰) are recorded from beds Cos2/3–160 to 172 (Fig. 7) and Cos4–108 to 208 (Fig. 8), which correspond to the lower *Serpentinum* Zone of the lower Toarcian. In detail, the uppermost Pliensbachian to middle Toarcian bulk carbonate C-isotopic record (Figs. 7, 8) is characterized by a first minor negative trend (0.4‰ in magnitude) starting in the uppermost Pliensbachian and crossing the Pliensbachian-Toarcian boundary (values from ca. 0.7‰ down to 0.3‰ in Cos2/3, and from ca. 0.8‰ down to 0.4‰ in Cos4), interrupted by a positive shift of 1.4‰ of magnitude in the lower *Tenuicostatum* Zone (values up to 1.8‰ in Cos4; Fig. 8). This positive shift is best defined in the Cos4 section, because in the equivalent position in the Cos2/3 section the interval is represented by only one data point, due to poor exposition and poorer density of sampling (Fig. 7). It is followed by a larger negative CIE of ca. 1.9‰ of amplitude (values from 1.8‰ down to −0.1‰ in Cos4) for the upper *Tenuicostatum* and lowermost *Serpentinum* zones (Fig. 8). From there, the $\delta^{13}C$ turns toward higher values of up to 2.5‰ in the lower-middle part of the *Serpentinum* Zone (*Elegantulum* Subzone). From bed Cos4–212 (Fig. 8) in the upper part of the *Serpentinum* Zone upwards into the *Bifrons* Zone, the $\delta^{13}C_{bulk\text{-}carb}$ values return to lower values, but in general still above +1.2‰.

The bulk $\delta^{18}O_{bulk\text{-}carb}$ record shows more uniform values, ranging

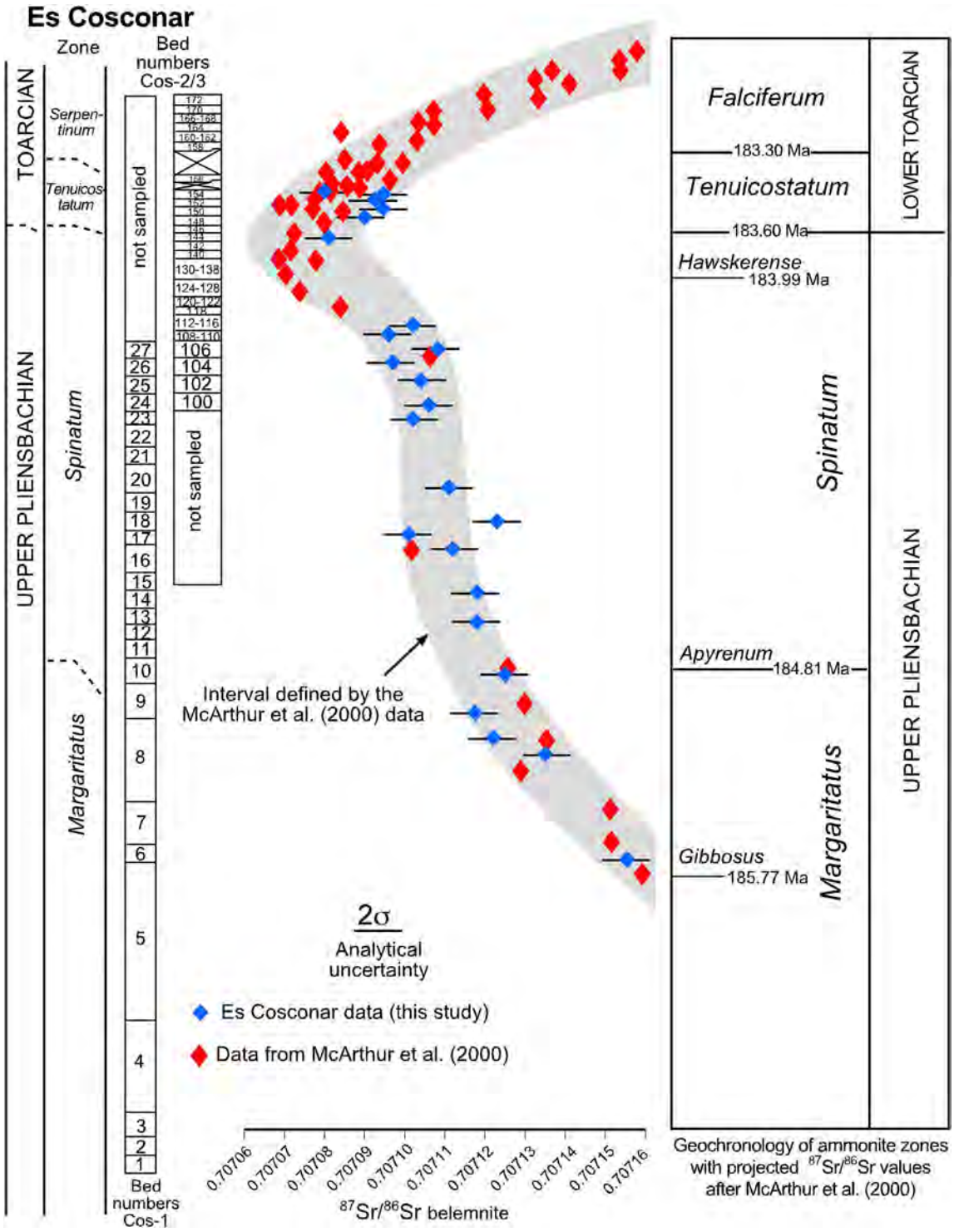

Fig. 6. Strontium-isotope stratigraphy based on diagenetically screened belemnite calcites from Es Cosconar (Majorca) plotted against stratigraphic levels and the $^{87}Sr/^{86}Sr$ data, ammonite biochronozones and numerical ages from McArthur et al. (2000).

between −2.4‰ and −4.8‰ (see Supplementary Information, Table S3). In general, lower $\delta^{18}O_{bulk\text{-}carb}$ values are registered for the lower part of the succession, corresponding also with the interval with the lowest $\delta^{13}C_{bulk\text{-}carb}$ values in the *Margaritatus* Zone of the upper Pliensbachian. This part of the succession is interpreted to be overprinted by diagenesis; thus the isotopic data from this part were excluded for subsequent interpretation and are not represented in Fig. 7. The uppermost Pliensbachian *Spinatum* Zone exhibits rather constant $\delta^{18}O_{bulk\text{-}carb}$ values around −3‰. These values are maintained across the Pliensbachian-Toarcian boundary and slightly decrease (down to −4.3‰) for the *Tenuicostatum* Zone of the lower Toarcian up to the *Bifrons* Zone (middle Toarcian).

4.4.2. Belemnite calcite carbon and oxygen isotopes

Cross-plot of $\delta^{18}O$ vs. $\delta^{13}C$ data from the analyzed belemnite samples (Fig. 5) shows a weak negative correlation, indicative of the insignificant diagenetic overprint upon the belemnite isotopic values

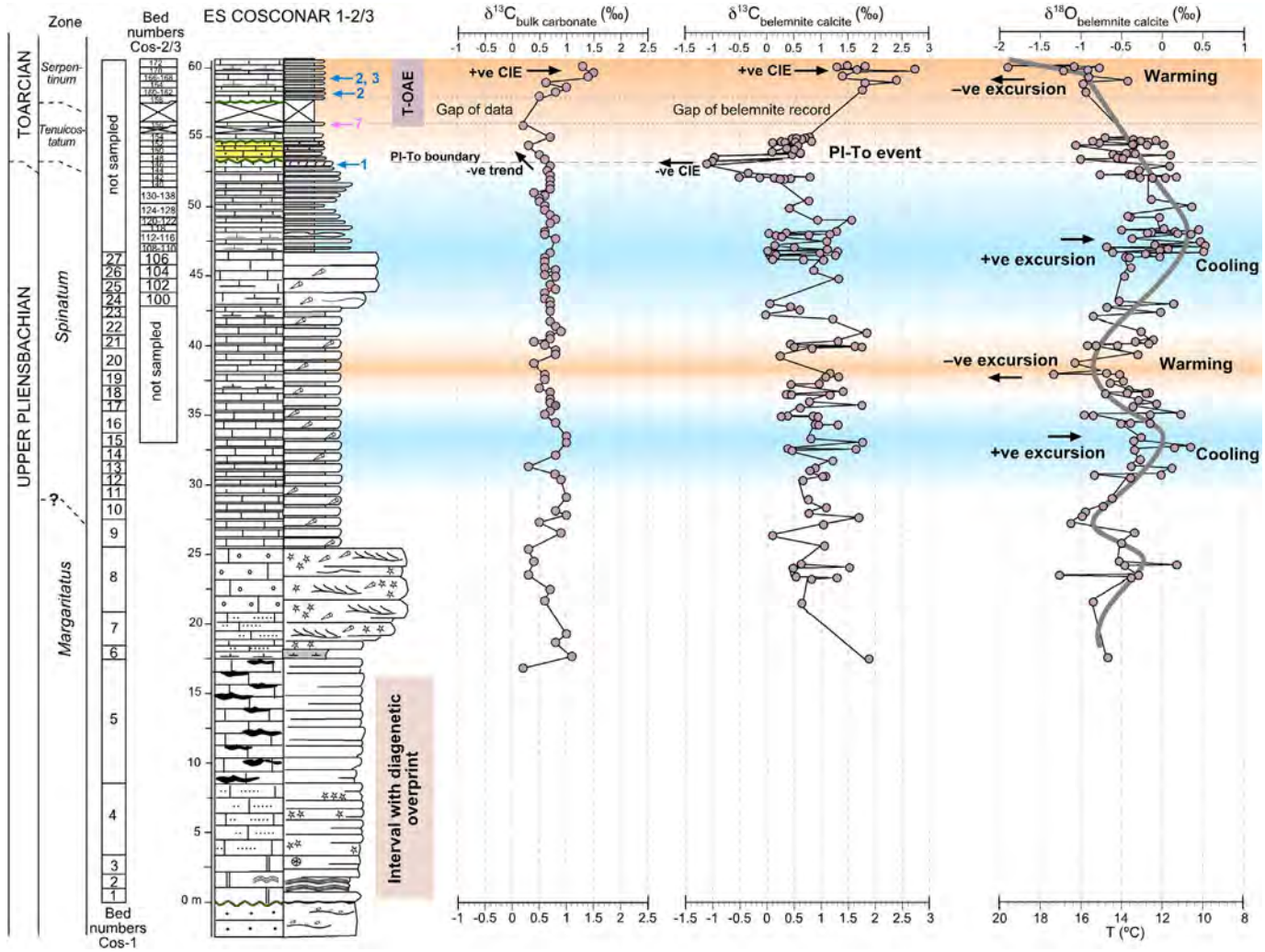

Fig. 7. Composite lithological profile of the Es Cosconar 1 (Cos1) and Es Cosconar 2 and 3 (Cos2/3) sections showing bulk carbonate and belemnite isotope stratigraphies, along with variations of estimated seawater temperatures through the late Pliensbachian–early Toarcian interval. Temperature estimates are based on $\delta^{18}O$ values using the formula of Anderson and Arthur (1983), and assuming an original $\delta^{18}O$ of non-glacial Jurassic seawater of −1‰ SMOW. Arrows with numbers 1, 2, 3 and 7 represent the position of key ammonite and brachiopod data; see Fig. 4 for the key of the numbers.

(Marshall, 1992). The $\delta^{13}C_{bel}$ isotope values range from about −1.2 to +2.7‰ (Supplementary Information, Table S1). The data obtained for the upper Pliensbachian scatter from −0.4‰ to +2.3‰, showing a trend toward in general more positive values in the *Spinatum* Zone, around beds Cos1–20 to 22 (Fig. 7). From bed Cos1–22 in the *Spinatum* Zone to the Pliensbachian-Toarcian boundary, around beds Cos2/3–142 to 146, the values show a trend to decrease, reaching a minimum of −1.2‰ for the Pliensbachian-Toarcian transition and lowermost *Tenuicostatum* Zone of the lower Toarcian (negative CIE, Fig. 7). The values rise rapidly, recovering positive values between 0 and +1‰, in the middle part of the *Tenuicostatum* Zone of the lower Toarcian. There is a gap of data (lack of exposure and belemnite samples in the field) for the upper *Tenuicostatum* Zone and the transition between the *Tenuicostatum* and *Serpentinum* zones of the lower Toarcian (Fig. 7). Above this gap, belemnite data collected for the *Serpentinum* Zone exhibit a pronounced positive CIE with values above +1.2‰ and up to +2.7‰ (Fig. 7).

The obtained $\delta^{18}O_{bel}$ isotope values range between +0.4 and −1.9‰ (Supplementary Information, Table S2). The $\delta^{18}O_{bel}$ isotope record is marked by several positive and negative excursions throughout the studied interval (Fig. 7). In the upper part of the *Margaritatus* Zone, coinciding with the facies change to high-energy cross-bedded grainstones of bed Cos1–8 (Fig. 7), the $\delta^{18}O_{bel}$ isotopes exhibit positive values up to +0.2‰ (mean − 0.5‰). The transition between the *Margaritatus* and *Spinatum* zones is characterized by a shift toward more negative values (down to −1.1‰, mean − 0.8‰). The *Spinatum* Zone record displays two positive O-isotope excursions punctuated by a negative excursion toward the middle part (values down to −1.4‰ around bed Cos1–19; Fig. 7). The upper positive excursion is the most prominent and displays values up to +0.5‰ (mean + 0.4‰) around beds Cos2/3–108 to 126 (Fig. 7). Following this maximum in the upper part of the *Spinatum* Zone, the O-isotopes show a progressive decrease throughout the Pliensbachian-Toarcian transition and into the *Tenuicostatum* Zone, recording a minimum (negative excursion) for the *Serpentinum* Zone of the lower Toarcian (Fig. 7).

5. Discussion

5.1. Sedimentary T/R sequences

Above the lower Pliensbachian (Carixian) deltaic siliciclastics of the Es Racó Member, the upper Pliensbachian (Domerian) to middle Toarcian succession of the Es Cosconar section shows a long-term deepening-upward facies evolution from peritidal laminated limestones at the bottom of the succession, to shallow open platform grainstones, outer platform packstone-wackestone and finally hemipelagic marls-limestone alternations in the upper part (Fig. 4). This succession can be

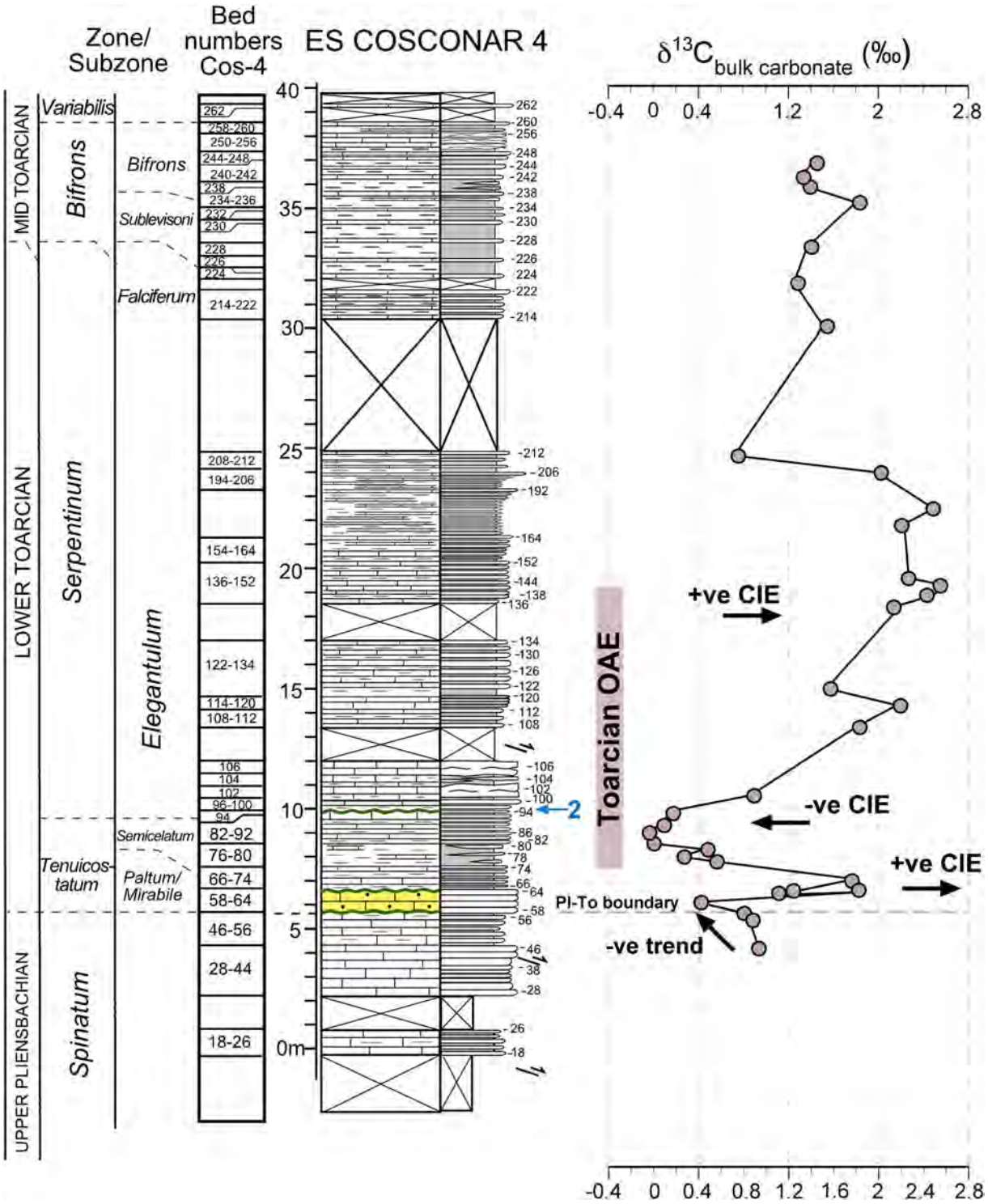

Fig. 8. Lithological profile of the Es Cosconar 4 (Cos4) section, with representation of bed numbers, ammonite chronozones and subchronozones and bulk carbonate carbon isotope stratigraphy. Arrow with number 2 represents the position of key brachiopod data; see Fig. 4 for the key of the numbers.

interpreted as the expression of the major global transgressive event at the scale of a first-order subcycle (Liassic or Ligurian cycle) that affected the epeiric seas of the European basins (Jacquin and De Graciansky, 1998; Hallam, 2001).

This long-term transgressive phase can be subdivided into four decametric-scale transgressive-regressive (T/R) facies cycles based on outcrop sedimentological facies interpretation and recognition of unconformities. The T/R facies cycles are comprised by a transgressive phase with a deepening-upward facies trend and a regressive phase that shows upward shallowing of facies (Fig. 4). The cycle T/R-1 corresponds to the *Margaritatus* Zone (beds Cos1–1 to 8; Fig. 4). Its lower boundary is located on top of the Es Racó Member, and is represented by a sharp shift from pebbly siliciclastic fluvio-deltaic deposits to shallow marine carbonate deposits. The transgressive part of the cycle is constituted by a deepening-upward trend from peritidal limestones to subtidal packstones-grainstones. Maximum flooding is located at bed Cos1–6, made of open marine marls with belemnites (Fig. 4). The regressive part of the cycle (beds Cos1–7 to 8) is represented by the rapid

change to high-energy crinoidal cross-bedded grainstones. The cycle T/R-2 (lower-middle *Spinatum* Zone) is represented in its lower transgressive hemicycle by open platform limestones with belemnites, brachiopods and pectinid bivalves. The upper part of the cycle (beds Cos1–24 to 27) shows a regressive trend evidenced by the relative shallowing and thickening of the limestones beds, which are richer in bioclasts, brachiopods and pectinid bivalves. Above this interval, the transgressive hemicycle of the following T/R-3 cycle (uppermost Pliensbachian, upper *Spinatum* Zone) shows dominance of outer ramp/platform facies. Toward the upper part, the regressive hemicycle (R3) becomes more bioclastic and silty-sandy, with abundant bioturbation and small planispiral gastropods (Fig. 4). The top of the cycle T/R-3 is represented by a major transgressive surface, highly bioturbated, over which occurs the onset of hemipelagic deposition of ammonites-rich, marl-limestone alternations of the Toarcian (Fig. 4). This cycle boundary is located slightly above the Pliensbachian-Toarcian boundary. Finally, the transgressive hemicycle of the Toarcian cycle (T/R-4) culminates with maximum transgression in the *Bifrons* Zone (minimum limestone/marl ratio). The regressive part of this cycle has not been analyzed in this study.

Although in the Balearic Basin sedimentation since the Pliensbachian was primary controlled by rift tectonics (Álvaro et al., 1989), comparison of the T/R facies cycles identified in the Es Cosconar section with coeval successions in other basins shows reasonable agreement for some of the sequences. A feature common to many basins is the regressive trend of the sequence T/R-2 in the *Spinatum* Zone, which is characterized by a period of widespread sea-level lowstand. This regressive trend has been related to cooler climatic conditions that preceded the climatic warming of the early Toarcian (Price, 1999; Korte et al., 2015). The regressive event of the upper hemicycle of the sequence T/R-2, has also been recognized in other basins of the Iberian Plate such as the Basque-Cantabrian and Iberian basins (Quesada et al., 2005; Gómez and Goy, 2005; Rosales et al., 2006; Val et al., 2017). The top boundary of the sequence T/R-3, which is close to the Pliensbachian-Toarcian boundary, could be correlated with a flooding surface in the European and Tethyan basins. Above this boundary the deepening and transgressive event of the lower Toarcian (T/R-4) is also other global feature of major sea-level rise that is associated with the spread of anoxic conditions and black shales in European basins (Hallam, 2001).

5.2. Oxygen isotope records and paleotemperatures

The $\delta^{18}O_{bel}$ values, which have been previously tested for diagenetic alteration, are regarded as recording original $\delta^{18}O$ composition of the ambient seawater (following reason given in Sælen et al., 1996; Podlaha et al., 1998; Rosales et al., 2001, 2004a; Wierzbowski, 2004; Harazim et al., 2012; Price et al., 2012; Korte et al., 2015; Gómez et al., 2016a, among others). The variations observed in the $\delta^{18}O_{bel}$ composition may have responded to changes in either seawater temperature or water isotopic composition. Assuming a constant seawater isotopic composition throughout the analyzed time span, the temperature dependence of the $\delta^{18}O_{bel}$ signal can be established by the temperature equation of Craig (1965), modified by Anderson and Arthur (1983):

$$T(^{\circ}C) = 16.0 - 4.14 \times (\delta_c - \delta_w) + 0.13 \times (\delta_c - \delta_w)^2 \quad (1)$$

where δ_C is the $\delta^{18}O$ composition of the belemnite calcite in ‰ relative to the V-PDB and δ_w is the $\delta^{18}O$ composition of precipitation water in ‰ relative to SMOW. Paleotemperatures were calculated from the $\delta^{18}O_{bel}$ values assuming a normal marine salinity and a commonly accepted original $\delta^{18}O_{water}$ composition for the ice-free Jurassic seas of −1‰ SMOW. The calculated paleotemperatures range between 10.2 °C and 19.9 °C (Supplementary Information, Table S2), with minimum temperatures recorded in the *Spinatum* Zone of the upper Pliensbachian and maximum temperatures in the *Serpentinum* Zone of the lower Toarcian (Fig. 7). Due to the gap of belemnite samples, no temperature estimates can be reported for the upper part of the *Tenuicostatum* Zone. The use of other temperature equations such as that of Friedman and O'Neil (1977) reduces all the temperature estimates to 6.2 °C cooler. These later temperatures are considered too low to be representative of platform habitats, therefore the estimates deduced from the Anderson and Arthur (1983) equation are considered more realistic. Nevertheless, these seawater paleotemperatures should be accepted with caution due to several reasons. First, because belemnites are extinct organisms and their exact isotope-temperature dependence remains somewhat speculative. Second, because the invariable δ_w value of −1‰ SMOW, usually assumed for ice-free seawater, may have varied regionally or temporally over the studied time interval. A range between −0.1‰ and 1.2‰ has been estimated by some authors (Bernasconi et al., 2011; Armendáriz et al., 2013). Finally, because the highly porous ultrastructure of the belemnite rostra may have been filled with abiotic syntaxial calcite overgrowths shortly after the death of the organism or even while the organism was still alive (Hoffmann et al., 2016; Benito et al., 2016), adding some uncertainty about the significance of these isotopic signals.

The range of Early Jurassic (late Pliensbachian–early Toarcian) paleotemperatures inferred for the Balearic Basin (10.2 to 19.9 °C) matches well with estimates from contemporaneous successions in other neighbouring basins of the Subboreal realm, such as the Grands Causses Basin in France (11 to 21 °C; Harazim et al., 2012), and the Basque-Cantabrian (9 to 26 °C; Rosales et al., 2001, 2004a) and Asturian (11.6 to 21 °C; Gómez et al., 2008) basins in northern Spain. In the Balearic Basin, the upper Pliensbachian *Spinatum* Zone is characterized by a trend to progressive cooler paleotemperatures (down to 10 °C, mean 13 °C), interrupted by an intermediate warming event where temperatures reached up to 17 °C (mean 14 °C). The coolest temperatures (down to 10 °C, mean 12 °C) are registered toward the upper part of the *Spinatum* Zone (beds Cos2/3–104 to 138; Fig. 7). Late Pliensbachian cooling, with similar mean paleotemperatures in an equivalent biostratigraphic position, has been evidenced also from belemnite records of basins in northern Spain (Rosales et al., 2001, 2004a; van de Schootbrugge et al., 2005b; Gómez et al., 2008, 2016a), Germany (Bailey et al., 2003) and France (Harazim et al., 2012), from belemnite and brachiopod records of the Iberian Basin in central Spain (Gómez et al., 2008; Val et al., 2017), and from brachiopod records of the Lusitanian Basin (Suan et al., 2010). In the Balearic Basin, this cooling event is followed by a trend toward progressive warmer temperatures across the Pliensbachian–Toarcian transition, reaching a maximum (up to ~20 °C, mean 16.2 °C) during the *Serpentinum* Zone of the lower Toarcian (Fig. 7). This represents an increase of mean seawater temperatures of about 4 °C. This warming event, which has been widely detected contemporaneously in many other European and Peri-Tethyan basins, has been referred to as the early Toarcian Rapid Warming or Superwarming linked to the T-OAE (see reviews in Jenkyns, 2003; Gómez et al., 2016a). An alternative interpretation to warming has been offered to explain the widespread $\delta^{18}O_{bel}$ shift toward lighter values observed in the early Toarcian. This alternative relates the isotopic shift to a change in the paleoecology of belemnites, as they may have shifted their life habitats from cold bottom waters to warmer surface waters as a response to expanding bottom sea anoxia during the T-OAE (Ullmann et al., 2014).

5.3. Carbon isotope records and the impact of the T-OAE

A composite upper Pliensbachian–middle Toarcian bulk-carbonate carbon isotope stratigraphy of the Es Cosconar section is shown in Fig. 9 and it is compared to the belemnite carbon isotope record. The limited exposure of the Toarcian portion of the succession in the section Cos2/3, and the possibility that some strata may be missing in one or both sections associated to the unconformities of base and top of the lowermost Toarcian yellowish-tan sandy calcarenites (Fig. 4), preclude a bed by bed correlation between Cos2/3 and Cos4 for the uppermost

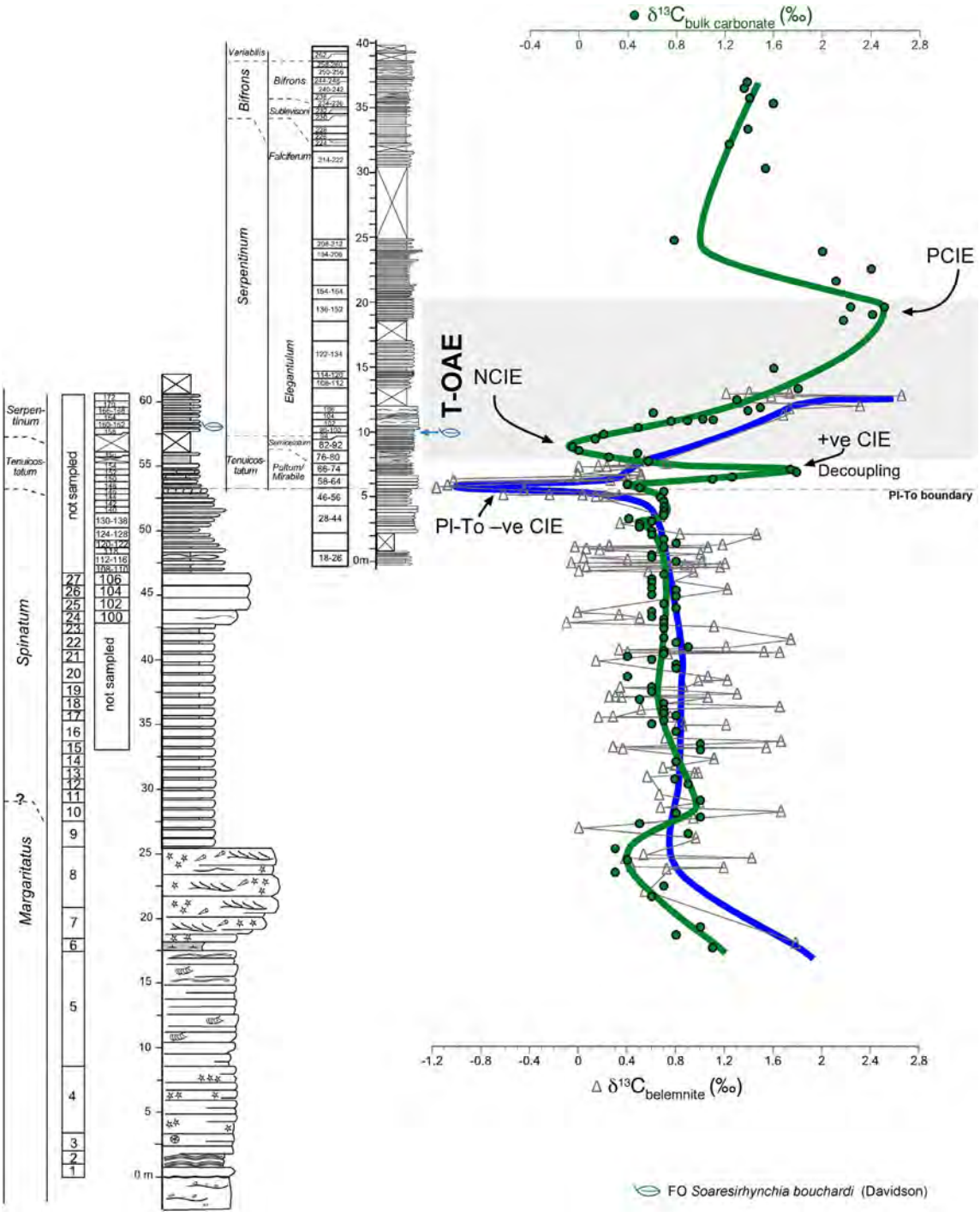

Fig. 9. Comparative bulk carbonate and belemnite carbon isotope records for the upper Pliensbachian–middle Toarcian of Es Cosconar (Majorca, Balearic Basin). The Pliensbachian-Toarcian transition is characterized in the belemnite record by a negative CIE (Pl-To –ve CIE) of about 2‰ of magnitude. The bulk carbonate carbon isotope record shows a minor negative trend across the Pliensbachian-Toarcian boundary followed by a positive shift (+ ve CIE) in the lower *Tenuicostatum* Zone of the Toarcian. The upper *Tenuicostatum* to lowermost *Serpentinum* zones register a negative CIE (NCIE) followed by a positive CIE (PCIE) in the middle *Serpentinum* Zone. Blue line: belemnite carbon isotope curve. Green line: bulk carbonate carbon isotope curve. (For interpretation of the references to colour in this figure legend, the reader is referred to the web version of this article.)

Pliensbachian–lowermost Toarcian interval of overlap between the two sections. For this reason, the composite bulk carbonate carbon isotope record was constructed using for the Pliensbachian only isotopic data from section Cos2/3, and for the lowermost Toarcian only isotopic data from section Cos4, adopting the base of the yellowish-tan sandy calcarenites as the surface of correlation (Fig. 4). Thus, for this interval there is not overlap of records between the two sections that could mix up data from different strata, adding potential noise.

The comparison of the resulting bulk carbonate and belemnite carbon isotope records shows that in the upper Pliensbachian both records are characterized by an initial trend toward decreasing values in the upper part of the *Margaritatus* Zone that are followed by near constant mean values through the *Spinatum* Zone, although less obvious in the belemnite record, with a high range of inter-specimen variability of about 1‰ (Fig. 9). The bulk carbonate $\delta^{13}C$ record across the Pliensbachian-Toarcian transition and lower Toarcian is marked by four isotopic events (Fig. 9). After a first minor, short-term negative shift registered through the Pliensbachian-Toarcian boundary, the lower

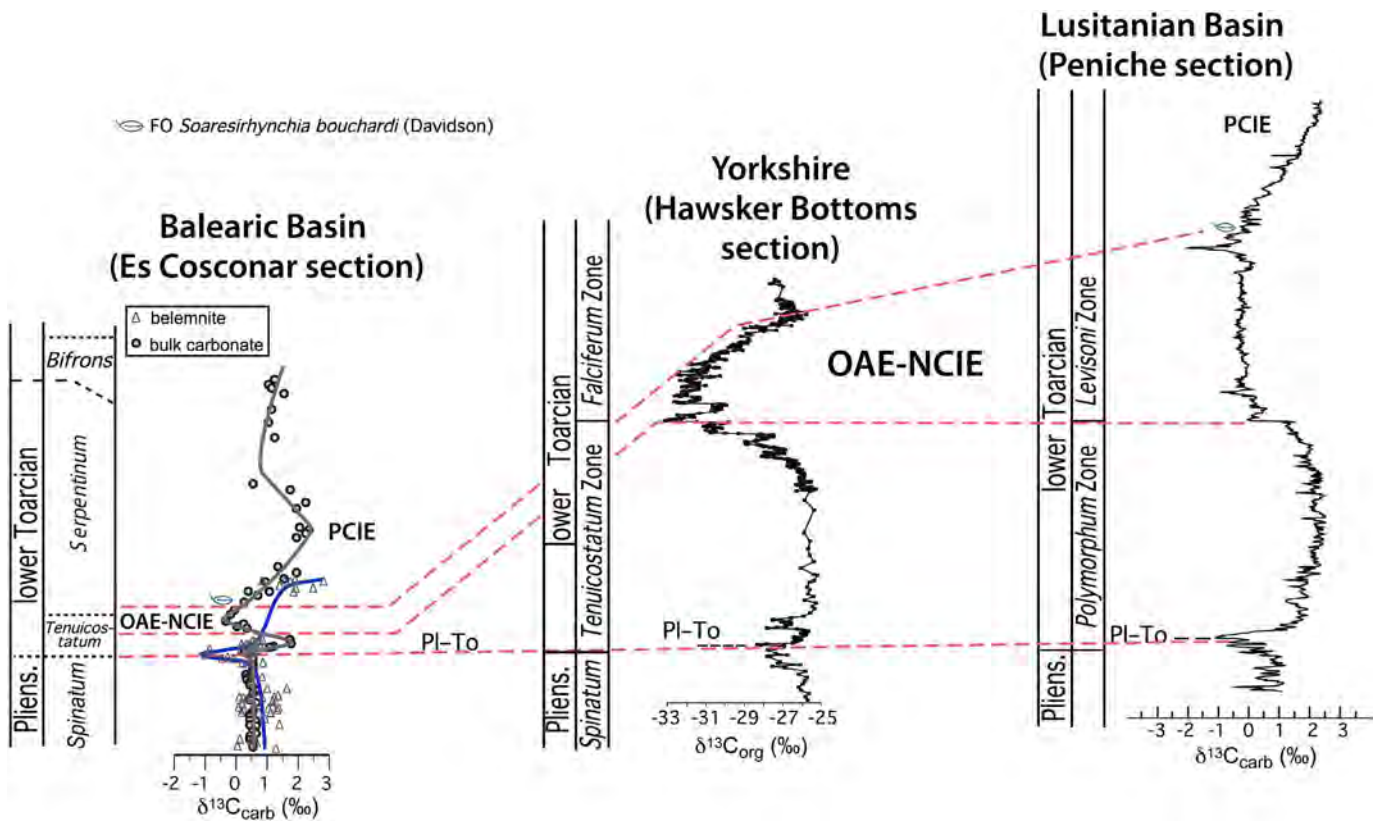

Fig. 10. Attempt of chemostratigraphic correlation of the belemnite and bulk carbonate carbon isotope records of the Es Cosconar section (Balearic Basin) with the two well-documented uppermost Pliensbachian–lower Toarcian carbon isotope chemostratigraphies of the Yorkshire (Boreal realm) and Lusitanian (Tethyan realm) basins. Note that the Yorkshire and Lusitania records correspond to much more expanded sections compared to Es Cosconar. Source of data: Es Cosconar (this study), Yorkshire (Hawsker Bottoms section) from Littler et al. (2010), Lusitania (Peniche section) from Hesselbo et al. (2007).

Tenuicostatum Zone is characterized by a prominent and rapid positive CIE (Fig. 9). It is followed by a negative CIE in the upper *Tenuicostatum* Zone and lowermost *Serpentinum* Zone (Fig. 9). The fourth carbon isotopic event is a pronounced positive shift of about 2.5‰ in the lower-middle *Serpentinum* Zone (Fig. 9). The equivalent belemnite carbon isotope profile, with significantly less inter-specimen variability than that of the Pliensbachian, records two carbon isotopic events. The first is a prominent negative CIE across the Pliensbachian-Toarcian transition (Pl-To –ve CIE in Fig. 9). It is followed by a return, in the lower *Tenuicostatum* Zone, to the mean values of the upper Pliensbachian, coinciding with the positive CIE of the bulk carbonate record. From there, there is a gap of data in the belemnite record, which matches with the position of the main negative CIE in the bulk carbonate record. The next isotopic event in the belemnite record is a pronounced positive shift in the lower-middle *Serpentinum* Zone, comparable to that observed in the bulk carbonate at the same stratigraphic position (Fig. 9).

Previous studies of carbon isotope records of European and Tethyan sections have shown the existence of two short-term negative CIEs during the early Toarcian (Fig. 10), the first around the Pliensbachian-Toarcian boundary (Pl-To event) (e.g. Hesselbo et al., 2007; Suan et al., 2010; Littler et al., 2010; Hesselbo and Pieńkowski, 2011; Bodin et al., 2016; Gómez et al., 2016a; Ait-Itto et al., 2017), and the second from the upper *Tenuicostatum* to the lower *Serpentinum/Levisoni/Falciferum* Zone (e.g. Röhl et al., 2001; van de Schootbrugge et al., 2005b; Hesselbo et al., 2000, 2007; Hermoso et al., 2009, 2014; Suan et al., 2010; Al-Suwaidi et al., 2010; Hesselbo and Pieńkowski, 2011; Izumi et al., 2012; Montero-Serrano et al., 2015). Because of a clear wide expression of the later in different carbon reservoirs such as bulk-rock carbonates, organic matter, wood and brachiopods, it has been interpreted to represent a major global disturbance of the carbon cycle, and its expression has been postulated as a feature that characterize the onset of the T-OAE (Hesselbo et al., 2000). To explain these negative isotopic anomalies, an increase or release of isotopically-light carbon into the system is required. The variety of mechanisms put forward to explain the supply of isotopically-light carbon have been discussed widely in literature, but they could be summarized in five: 1) release of methane from gas hydrate dissociation, 2) decomposition or burning of wetlands or older organic rocks and coals by thermal metamorphism, 3) degassing CO_2 from LIPs in the Karoo-Ferrar LIP province, 4) presence of secondary carbonate precipitated from methanogenesis and sulphate reduction during diagenesis of the organic matter, and 5) the so-called Küspert model, which implies the recycling or upwelling of ^{12}C–rich bottom waters to the surface in a highly stratified water column (e.g. Küspert, 1982; Hesselbo et al., 2000; Jenkyns, 2003; McElwain et al., 2005; Cohen et al., 2007; Gröcke et al., 2009).

In the case of the Balearic Basin, it is significant that belemnites of the Es Cosconar section show a pronounced and short negative CIE for the levels that cross the Pliensbachian-Toarcian boundary (Fig. 9), which can be correlated to the first negative carbon isotope event recognized in other sections such as Yorkshire and Peniche in Portugal (Pl-To in Fig. 10). It is worth noting that this is the first time in our knowledge that this negative isotopic excursion is well documented with a prominent peak in belemnite calcites, because in other studies the negative excursion is not or is only weakly expressed in the calcite of the belemnites (van de Schootbrugge et al., 2005a; Hesselbo et al., 2007; Littler et al., 2010; Gómez et al., 2016b; Ait-Itto et al., 2017), although it does in the organic matrix of the belemnites (Ullmann et al., 2014).

In Majorca, this negative shift in the belemnite record and the rapid return in the lower *Tenuicostatum* Zone to the mean values of the upper Pliensbachian, are coeval in the bulk carbonate record to a minor negative shift followed by a marked positive isotopic excursion (Fig. 9). As

belemnites were presumably nektobenthonic, the decoupling between both carbonate carbon reservoirs at this time suggests strong water stratification during this event. Belemnites are interpreted to have recorded isotopically-light, near bottom water conditions, whereas the bulk carbonate (micrite) record may represent precipitation from isotopically heavier surface waters. These results are also inconsistent with the Küspert model (upwelling) that would have resulted in isotopically lighter bulk-rock values. Recently, Bodin et al. (2016) have proposed an alternative for the interpretation of other observed decoupling associated to these isotopic events, based on changes in the composition of the bulk carbonate fraction and the rate of carbonate exported from neritic environments. As the neritic micrite tends to show more positive $\delta^{13}C$ values than the ooze micrite produced by pelagic organisms (Swart and Eberli, 2005), the input of neritic micrite and mixing of these two fractions with different $\delta^{13}C$ values would rise the bulk carbonate $\delta^{13}C$ signal compared to that of belemnites (Bodin et al., 2016). In the Es Cosconar section, the Pliensbachian-Toarcian transition to lowermost *Tenuicostatum* Zone correspond to the late regressive part of the facies cycle T/R-3 (Fig. 4), suggesting low relative sea level at this time. This situation may have enhanced the export of neritic micrite to the outer platform environment due to a reduction of accommodation on the shallow shelf (e.g. Dix et al., 2005), resulting in the positive shift of the bulk carbonate record and the more positive carbon isotope values of the bulk carbonate compared to belemnites. This is supported by a coeval lithological change in the Es Cosconar section to more bioclastic deposits (Fig. 4), suggesting higher rates of carbonate shedding from the platform environments that may have masked the oceanic isotopic signal by local processes.

The negative CIE observed in the bulk carbonate record spanning the upper *Tenuicostatum* and lowermost *Serpentinum* zones, is not captured in the belemnite isotopic record of Es Cosconar because this interval corresponds with a gap of data (lack of belemnites recollected from this interval in the Cos 2/3 section; Fig. 7). Thus, its representation in belemnites of the Balearic Basin still remains unresolved. The position of this negative isotopic event in bulk carbonate correlates with the postulated global negative CIE that typifies the onset of the T-OAE in contemporaneous strata of other basins (Fig. 10). This is supported by the stratigraphic position where the first occurrence of *S. buchardi* was found in the sections of Es Cosconar (Cos2/3 and Cos4; Figs. 4, 7, 8, 9). In Spain and Portugal, including Peniche, this species is generally the first brachiopod to occur just above an extinction boundary that coincides with the termination of the negative CIE (Fig. 10), representing the recovery after an important biotic crisis (Suan et al., 2010; García Joral et al., 2011; Pittet et al., 2014). Therefore, the position of the first occurrence (FO) of *S. buchardi* in Es Cosconar reinforces the interpretation that the negative CIE observed thought the upper *Tenuicostatum* to the lowermost *Serpentinum* zones in the Cos4 section correlates with that characterizing the T-OAE. In the Cos2/3 section this negative CIE is very likely located within the exposure gap and therefore missed here by the geochemical records (Fig. 9).

Comparison of the Es Cosconar results with other well-documented $\delta^{13}C_{carb}$ records shows that, in spite of some differences in absolute values and in the overall shape of the isotopic profiles (due to more reduced sedimentary rates and/or presence of hiatuses in Es Cosconar), the broad isotopic trends are similar to those documented in the classical section of Peniche and in other sections of Portugal (Hesselbo et al., 2007; Pittet et al., 2014). In Peniche (Fig. 10), the negative carbonate CIE of about 2‰ reported across the Pliensbachian-Toarcian boundary is recorded in the bulk carbonate of Es Cosconar as a very minor negative isotopic shift of about 0.3‰, and as a larger negative CIE of about 1.5‰ in the belemnite record. Following this event, in Peniche the $\delta^{13}C_{carb}$ values increase markedly through the *Polymorphum* Zone and shift to lower values toward the top of the biozone, defining a broad positive CIE of about 3‰ in magnitude (Fig. 10). This trend is reproduced also in the bulk carbonate isotope record of Es Cosconar as the positive excursion of about 1.4‰ observed in the lower *Tenuicostatum* Zone, although with obvious differences in shape due to the much more expanded record of Peniche compare to Es Cosconar. From these maximum values, the Es Cosconar record shows a rapid negative shift of about 1.9‰ across the *Tenuicostatum–Serpentinum* zones, which correlates with the ~2.5‰ negative CIE in average (maximum 3.5‰) defining the onset of the T-OAE in Peniche, in the lower *Levisoni* Zone (OAE-NCIE in Fig. 10). The lower magnitude of the negative CIEs documented from Es Cosconar compare to Peniche could be attributed to variations in the source of carbonate related to differences in their respective depositional environments. The Peniche section was deposited in a deeper environment with a presumably higher contribution of calcareous nannofossils and pelagic muds, which exhibit lighter $\delta^{13}C_{carb}$ values compared to the allochthonous platform-derived carbonate prevailing in shallower environments, such as Es Cosconar (intraplatform basin), which exhibit usually more positive $\delta^{13}C$ values (Pittet et al., 2014; Bodin et al., 2016)

Finally, the $\delta^{13}C_{carb}$ values rise again reaching maximum values in the lower-middle *Serpentinum* Zone or lower-middle *Levisoni* Zone in the Es Cosconar and Portugal records respectively. This positive CIE observed in both belemnite and bulk carbonate records, has been widely reproduced in many other shallow platform and hemipelagic carbonate carbon-isotope profiles around the world (e.g. Jiménez et al., 1996; Rosales et al., 2004a; Gómez et al., 2008; Suan et al., 2008; Sabatino et al., 2013; Arabas et al., 2017), and has been conventionally attributed to the massive burial of isotopically-light organic carbon in the bottom sea sediments during the T-OAE (Jenkyns and Clayton, 1997; Jenkyns, 1988). As consequence, the dissolved carbon of the ocean reservoir became progressively enriched in the heavier ^{13}C isotope, and this signal was fixed in the two carbonate carbon isotope reservoirs, belemnites and bulk carbonate.

6. Conclusions

The carbon and oxygen stable isotopic records of the late Pliensbachian to middle Toarcian are investigated for the first time in belemnites and bulk carbonate records of the Balearic Basin (westernmost Tethys). The chemostratigraphic records have been improved by the combination of biostratigraphic and $^{87}Sr/^{86}Sr$ geochronologic methods.

Data of the Balearic Basin confirm the existence of large oxygen-isotope fluctuations over the studied interval. They highlight the incidence of the already accepted late Pliensbachian cooling event and the warming event of the early Toarcian. This warming event, which has been widely detected contemporaneously in many other European and Tethyan basins, is interpreted to represent generalized raised seawater temperatures linked to the T-OAE.

The $\delta^{13}C_{bel}$ and $\delta^{13}C_{bulk\text{-}carb}$ records of the Es Cosconar section show four isotopic events or CIEs, which are consistent with carbon isotopic anomalies reported elsewhere for the latest Pliensbachian–early Toarcian. The first is a negative CIE around the Pliensbachian-Toarcian boundary (P-To event) best recognized in the belemnite record. The incidence of this isotopic event in the Balearic Basin is significant because this is the first time that a negative CIE of this age is clearly detected in belemnite calcites. It is followed in the lower *Tenuicostatum* Zone by a return to background values in the belemnite record, concomitant to a positive excursion in the $\delta^{13}C_{bulk\text{-}carb}$, suggesting strong water stratification and/or decoupling during this time. The positive shift observed in the bulk carbonate record may be associated to an increase of neritic mud export during a sea-level lowstand. A second negative CIE is observed in bulk carbonate records through the upper *Tenuicostatum* to lowermost *Serpentinum* zones, which is correlatable to the negative CIE characterizing the onset of the T-OAE in other sections. It is followed by a pronounced positive CIE for the *Serpentinum* Zone recorded in both belemnite and bulk carbonate records. The proven co-occurrence of these isotopic excursions in other basins from different

paleogeographic provinces gives support for their global significance.

Supplementary data to this article can be found online at https://doi.org/10.1016/j.palaeo.2018.02.016.

Acknowledgments

This work is a contribution to the project IGCP 655 "*Toarcian Oceanic Anoxic Event: Impact on marine carbon cycle and ecosystems",* and to the research projects CGL2015-66604-R and CGL2014-53548-P supported by the Spanish Ministry of Economy, Industry and Competitiveness. The authors thank to the IGME laboratories for the elemental analyses, to the laboratory of Geocronología y Geoquímica Isotópica (Universidad Complutense de Madrid) for the strontium isotopes, and to the Servicio General de Análisis de Isótopos Estables (Universidad de Salamanca) for the carbon and oxygen stable isotope analyses. The original manuscript benefited from the comments of two anonymous reviewers, and the constructive reviews of Guillaume Suan and editor-in-chief, Thomas Algeo.

References

Ait-Itto, F.-Z., Price, G.D., Ait Addi, A., Chafiki, D., Mannani, I., 2017. Bulk-carbonate and belemnite carbon-isotope records across the Pliensbachian-Toarcian boundary on the northern margin of Gondwana (Issouka, Middle Atlas, Morocco). Palaeogeogr. Palaeoclimatol. Palaeoecol. 466, 128–136.

Alberti, M., Fürsich, F.T., Pandey, D.K., Ramkumar, M., 2012. Stable isotope analyses of belemnites from the Kachchh Basin, western India: paleoclimatic implications for the Middle to Late Jurassic transition. Facies 58, 261–278.

Alméras, Y., Fauré, P., 2000. Les brachiopodes liasiques des Pyrénées. In: Paléontologie. Biostratigraphie. Paléobiogéographie et paléoenvironnement. Strata. 36. pp. 1–395.

Al-Suwaidi, A.H., Angelozzi, G.N., Baudin, F., Damborenea, S.E., Hesselbo, S.P., Jenkyns, H.C., Manceñido, M.O., Riccardi, A.C., 2010. First record of the early Toarcian oceanic anoxic event from the southern hemisphere, Neuquén Basin, Argentina. J. Geol. Soc. Lond. 167, 633–636. http://dx.doi.org/10.1144/0016-76492010-025.

Álvaro, M., Barnolas, A., Cabra, P., Comas-Rengifo, M.J., Fernández-López, S., Goy, A., Del Olmo, P., Ramírez Del Pozo, J., Simó, A., Ureta, M., 1989. El Jurásico de Mallorca (Islas Baleares). Cuad. Geol. Iber. 13, 67–120.

Anderson, T.F., Arthur, M.A., 1983. Stable isotopes of oxygen and carbon and their applications to sedimentologic and paleoenvironmental problems. In: Arthur, M.A., Anderson, T.F., Kaplan, I.R., Veizer, J., Land, L.S. (Eds.), Stable Isotopes in Sedimentary Geology, SEPM Short Course 10, pp. 1–151.

Arabas, A., Schlögl, J., Meister, Ch., 2017. Early Jurassic carbon and oxygen isotope records and seawater temperature variations: insights from marine carbonate and belemnite rostra (Pieniny Klippen Belt, Carpathians). Palaeogeogr. Palaeoclimatol. Palaeoecol. http://dx.doi.org/10.1016/j.palaeo.2017.06.007.

Armendáriz, M., Rosales, I., Quesada, C., 2008. Oxygen isotope and Mg/Ca composition of late Viséan (Mississippian) brachiopod shells from SW Iberia: Palaeoclimatic and palaeogeographic implications in northern Gondwana. Palaeogeogr. Palaeoclimatol. Palaeoecol. 268, 65–79.

Armendáriz, M., Rosales, I., Bádenas, B., Aurell, M., García-Ramos, J.C., Piñuela, L., 2012. High-resolution chemostratigraphic records from lower Pliensbachian belemnites: Palaeoclimatic perturbations, organic facies and water mass exchange (Asturian basin, northern Spain). Palaeogeogr. Palaeoclimatol. Palaeoecol. 333-334, 178–191.

Armendáriz, M., Rosales, I., Bádenas, B., Piñuela, L., Aurell, M., García-Ramos, J.C., 2013. An approach to estimate Lower Jurassic seawater oxygen- isotope composition using $\delta^{18}O$ and Mg/Ca ratios of belemnite calcites (early Pliensbachian, northern Spain). Terra Nova 25, 439–445.

Azañon, J.M., Galindo-Zaldivar, J., García-Dueñas, V., Jabaloy, A., 2002. Alpine tectonics II: Betic Cordillera and Balearic Islands. In: Gibbons, W., Moreno, T. (Eds.), The Geology of Spain. Geol. Soc, London, pp. 401–416.

Bailey, T.R., Rosenthal, Y., McArthur, J.M., van de Schootbrugge, B., Thirlwall, M.F., 2003. Paleoceanographic changes of the late Pliensbachian–early Toarcian interval: a possible link to the genesis of an oceanic anoxic event. Earth Planet. Sci. Lett. 212, 307–320.

Barnolas, A., Simó, A., 1984. Sedimentología. In: Barnolas, A. (Ed.), Sedimentología del Jurásico de Mallorca: Grupo Español del Mesozoico. IGME-CGS, Madrid (263 pp).

Bécaud, M., 2006. Les Harpoceratinae, Hildoceratinae et Paroniceratinae du Toarcien de la Vandée et des Deux-Sèvres (France). In: Documents des Laboratoires de Géologie Lyon. 162. pp. 1–245.

Benito, M.I., Reolid, M., 2012. Belemnite taphonomy (Upper Jurassic, western Tethys) part II: fossil-diagenetic analysis including combined petrographic and geochemical techniques. Palaeogeogr. Palaeoclimatol. Palaeoecol. 358-360, 89–108.

Benito, M.I., Reolid, M., Viedma, C., 2016. On the microstructure, growth pattern and original porosity of belemnite rostra: insight from calcitic Jurassic belemnites. J. Iber. Geol. 42, 201–226.

Bernasconi, S.M., Schmid, T.W., Grauel, A.E., Mutterlose, J., 2011. Clumped-isotope geochemistry of carbonates: a new tool for the reconstruction of temperature and oxygen isotope composition of seawater. Appl. Geochem. 26, S279–S280.

Bodin, S., Krencker, F.-N., Kothe, T., Hoffmann, R., Mattioli, E., Heimhofer, U., Kabiri, L., 2016. Perturbation of the carbon cycle during the late Pliensbachian–early Toarcian: new insight from high-resolution carbon isotope records in Morocco. J. Afr. Earth Sci. 116, 89–104.

Boulila, S., Hinnov, L.A., 2017. A review of tempo and scale of the early Jurassic Toarcian OAE: implications for carbon cycle and sea level variations. Newsl. Stratigr. 50, 363–389.

Cohen, A.S., Coe, A.L., Kemp, D.B., 2007. The late Palaeocene–early Eocene and Toarcian (Early Jurassic) carbon isotope excursions: a comparison of their time scales, associated environmental changes, causes and consequences. J. Geol. Soc. Lond. 164 (6), 1093–1108.

Colom, G., 1942. Sobre nuevos hallazgos de yacimientos fosilíferos del Lías medio y superior de la Sierra Norte de Mallorca. Bol. Real Soc. Esp. Hist. Nat. 60, 221–262.

Comas-Rengifo, M.J., Duarte, L.V., Félix, F.F., García Joral, F., Goy, A., Rocha, R.B., 2015. Latest Pliensbachian –early Toarcian brachiopod assemblages from the Peniche section (Portugal) and their correlation. Episodes 38, 2–8.

Craig, H., 1965. The measurement of oxygen isotope paleotemperatures. In: Tongiorgi, E. (Ed.), Stable Isotopes in Oceanographic Studies and Palaeotemperatures. Consiglio Nazionale delle Richerche, Laboratorio di Geologia Nucleare, Pisa, pp. 161–182.

Delance, J.H., 1969. Étude de quelques brachiopodes liasiques du Nord-Est de l'Espagne. In: Annales du Paléontologie. 55. Invertebres, París, pp. 1–54.

Dera, G., Neige, P., Dommergues, J.-L., Fara, E., Laffont, R., Pellenard, P., 2010. High-resolution dynamics of Early Jurassic marine extinctions: the case of Pliensbachian–Toarcian ammonites (*Cephalopoda*). J. Geol. Soc. Lond. 167, 21–33.

Dera, G., Brigaud, B., Monna, F., Laffont, R., Pucéat, E., Deconinck, J.-F., Pellenard, P., Joachimski, M.M., Durlet, Ch., 2011. Climatic ups and downs in a disturbed Jurassic world. Geology 39, 215–218.

Dercourt, J., Gaetani, M., Vrielynck, B., Barrier, E., Biju-Duval, B., Brunet, M.F., Cadet, J.P., Crasquin, S., Sandulescu, M. (Eds.), 2000. Atlas Peri Tethys, Palaeogeographical Maps. Vol. I–XX. CCGM/CGMW, Paris, pp. 1–269.

Dewey, J.F., Pitman, W.C., Ryan, W.B.F., Bonnin, J., 1973. Plate tectonics and the evolution of the Alpine system. GSA Bull. 84, 3137–3180.

Dix, G.R., James, N.P., Kyser, T.K., Bone, Y., Collins, L.B., 2005. Genesis and dispersal of carbonate mud relative to late Quaternary sea-level change along a distally-steepened carbonate ramp (northwestern shelf, Western Australia). J. Sediment. Res. 75, 665–678.

Dutton, A., Huber, B.T., Lohmann, K.C., Zinsmeister, W.J., 2007. High-resolution stable isotope profiles of a Dimitobelid belemnite: implications for paleodepth habitat and late Maastrichtian climate seasonality. PALAIOS 22, 642–650.

Elmi, S., Goy, A., Mouterde, R., Rivas, P., Rocha, R.B., 1989. Correlaciones bioestratigráficas en el Toarciense de la Península ibérica. Cuad. Geol. Iber. 13, 265–277.

Elmi, S., Rulleau, L., Gabilly, J., Mouterde, R., 1997. Toarcien. In: Cariou, E., Hantzpergue, P. (Eds.), Biostratigraphie du jurassique ouest-européen et mediterranéen. 17. Bulletin du Centre de recherchés Elf Exploration Production, Pau, pp. 25–36.

Fallot, P., 1922. Étude Géologique de la Sierra de Majorque. Libr. Polytech. Ch. Béranger, Paris (481 pp).

Fallot, P., 1932. Essais sur la répartition desterrains secundaires et tertiaires dans le domaine des Alpides espagnoles: Géol. Méd. Occid.: II. Le Lias. pp. 29–64.

Friedman, I., O'Neil, J.R., 1977. Compilation of stable isotope fractionation factors of geochemical interest. US Geol. Surv. Prof. Pap. 440 (12 pp).

Gahr, M.E., 2005. Response of lower Toarcian (Lower Jurassic) macrobenthos of the Iberian peninsula to sea-level changes and mass extinction. J. Iber. Geol. 31, 197–215.

García Joral, F., Goy, A., 2000. Stratigraphic distribution of the brachiopods from the Toarcian of the Iberian range (Spain) and its relation to depositional sequences. GeoResearch Forum. 6. pp. 381–386.

García Joral, F., Goy, A., 2009. The Toarcian (Lower Jurassic) brachiopods from Asturias (N Spain): stratigraphic distribution, critical events and palaeobiogeography. Geobios 42, 255–264.

García Joral, F., Gómez, J.J., Goy, A., 2011. Mass extinction and recovery of the early Toarcian (Early Jurassic) brachiopods linked to climate change in northern and central Spain. Palaeogeogr. Palaeoclimatol. Palaeoecol. 302, 367–380.

Gelabert, B., 1998. La estructura geológica de la mitad occidental de la Isla de Mallorca. Colección Memorias ITGE, Madrid (129 pp).

Gómez, J.J., Goy, A., 2005. Late Triassic and Early Jurassic palaeogeographic evolution and depositional cycles of the western Tethys Iberian platform system (eastern Spain). Palaeogeogr. Palaeoclimatol. Palaeoecol. 222, 77–94.

Gómez, J.J., Goy, A., 2011. Warming-driven mass extinction in the early Toarcian (Early Jurassic) of northern and central Spain. Correlation with other time-equivalent European sections. Palaeogeogr. Palaeoclimatol. Palaeoecol. 306, 176–195.

Gómez, J.J., Goy, A., Canales, M.L., 2008. Seawater temperature and carbon isotope variations in belemnites linked to mass extinction during the Toarcian (Early Jurassic) in central and northern Spain. Comparison with other European sections. Palaeogeogr. Palaeoclimatol. Palaeoecol. 258, 28–58.

Gómez, J.J., Comas-Rengifo, M.J., Goy, A., 2016a. Palaeoclimatic oscillations in the Pliensbachian (Early Jurassic) of the Asturian Basin (northern Spain). Clim. Past 12, 1199–1214.

Gómez, J.J., Comas-Rengifo, M.J., Goy, A., 2016b. The hydrocarbon source rocks of the Pliensbachian (Early Jurassic) in the Asturian Basin (northern Spain): their relationship with palaeoclimatic oscillations and gamma-ray response. J. Iber. Geol. 42, 259273.

Goy, A., Jiménez, A., Martínez, G., Rivas, P., 1988. Difficulties in correlating the Toarcian ammonite succession of the Iberian and Betic Cordilleras. In: 2nd International Symposium on Jurassic Stratigraphy, Lisboa, pp. 155–178.

Goy, A., Comas-Rengifo, M.J., Arias, C.F., García Joral, F., Gómez, J.J., Herrero, C.,

Martínez, G., Rodrigo, A., 1998. El tránsito Pliensbachiense/Toarciense en el Sector Central de la Rama Aragonesa de la Cordillera Ibérica (España). In: Cahiers de l'Université Catholique de Lyon. 10. pp. l59–179.
Gröcke, D.R., Rimmer, S.M., Yoksoulian, L.E., Cairncross, B., Tsikos, H., van Hunen, J., 2009. No evidence for thermogenic methane release in coal from the Karoo-Ferrar large igneous province. Earth Planet. Sci. Lett. 277, 204–212.
Hallam, A., 1997. Estimates of the amount and rate of sea-level changes across the Rhaetian-Hettangian and Pliensbachian-Toarcian boundaries (latest Triassic to early Jurassic). J. Geol. Soc. Lond. 154, 773–779.
Hallam, A., 2001. A review of the broad pattern of Jurassic sea-level changes and their possible causes in the light of current knowledge. Palaeogeogr. Palaeoclimatol. Palaeoecol. 167, 23–37.
Hallam, A., Wignall, P.B., 1999. Mass extinctions and sea-level changes. Earth Sci. Rev. 48, 217–250.
Harazim, D., van de Schootbrugge, B., Sorichter, K., Fiebig, J., Weug, A., Suan, G., Oschmann, W., 2012. Spatial variability of watermass conditions within the European Epicontinental seaway during the Early Jurassic (Pliensbachian–Toarcian). Sedimentology 60, 359–390. http://dx.doi.org/10.1111/j.1365-3091.2012.01344.x.
Harries, P.J., Little, C.T.S., 1999. The early Toarcian (Early Jurassic) and the Cenomanian–Turonian (Late Cretaceous) mass extinctions: similarities and contrasts. Palaeogeogr. Palaeoclimatol. Palaeoecol. 154, 39–66.
Hermoso, M., Le Callonnec, L., Minoletti, F., Renard, M., Hesselbo, S.P., 2009. Expression of the early Toarcian negative carbon-isotope excursion in separated carbonate microfractions (Jurassic, Paris Basin). Earth Planet. Sci. Lett. 277, 194–203.
Hermoso, M., Minoletti, F., Rickaby, R.E.M., Hesselbo, S.P., Baudin, F., Jenkyns, H.C., 2012. Dynamics of a stepped carbon-isotope excursion: ultra high-resolution study of early Toarcian environmental change. Earth Planet. Sci. Lett. 319-320, 45–203.
Hermoso, M., Delsate, D., Baudin, F., Le Callonnec, L., Minoletti, F., Renard, M., Faber, A., 2014. Record of early Toarcian carbon cycle perturbations in a nearshore environment: the Bascharage section (easternmost Paris Basin). Solid Earth 5, 793–804.
Hesselbo, S.P., Pieńkowski, G., 2011. Stepwise atmospheric carbon-isotope excursion during the Toarcian oceanic anoxic event (Early Jurassic, Polish Basin). Earth Planet. Sci. Lett. 301, 365–372.
Hesselbo, S.P., Gröcke, D., Jenkyns, H.C., Bjerrum, C.J., Farrimond, P., Morgans Bell, H.S., Green, O.R., 2000. Massive dissociation of gas hydrate during a Jurassic oceanic anoxic event. Nature 406, 392–395.
Hesselbo, S.P., Jenkyns, H.C., Duarte, L.V., Oliveira, L.C.V., 2007. Carbon-isotope record of the Early Jurassic (Toarcian) oceanic anoxic event from fossil wood and marine carbonate (Lusitanian Basin, Portugal). Earth Planet. Sci. Lett. 253, 455–470.
Hoffmann, R., Richter, D.K., Neuser, R.D., Jöns, N., Linzmeier, B.J., Lemanis, R.E., Fusseis, F., Xiao, X., Immenhauser, A., 2016. Evidence for a composite organic-inorganic fabric of belemnite rostra: implications for palaeoceanography and palaeoecology. Palaeogeogr. Palaeoclimatol. Palaeoecol. 341, 203–215.
Huang, Ch., Hesselbo, S.P., 2014. Pacing of the Toarcian anoxic event (Early Jurassic) from astronomical correlation of marine sections. Gondwana Res. 25, 1348–1356.
Izumi, K., Miyaji, T., Tanabe, K., 2012. Early Toarcian (Early Jurassic) oceanic anoxic event recorded in the shelf deposits in the northwestern Panthalassa: evidence from the Nishinakayama Formation in the Toyora area, west Japan. Palaeogeogr. Palaeoclimatol. Palaeoecol. 315–316, 100–108.
Jacquin, T., De Graciansky, P.C., 1998. Major transgressive/regressive cycles: the stratigraphic signature of European basin development. In: De Graciansky, P.C., Hardenbol, J., Jacquin, T., Vail, P.R. (Eds.), Mesozoic and Cenozoic Sequence Stratigraphy of European Basins. Special Publications 60. Society of Economic Paleontologists and Mineralogists, pp. 15–29.
Jenkyns, H.C., 1988. The early Toarcian (Jurassic) anoxic event: stratigraphic, sedimentary and geochemical evidence. Am. J. Sci. 288, 101–151.
Jenkyns, H.C., 2003. Evidence for rapid climate change in the Mesozoic–Palaeogene greenhouse world. Philos. Trans. R. Soc. Lond. A 361, 1885–1916.
Jenkyns, H.C., 2010. Geochemistry of oceanic anoxic events. Geochem. Geophys. Geosyst. 11, Q03004. http://dx.doi.org/10.1029/2009GC002788.
Jenkyns, H.C., Clayton, C.J., 1997. Lower Jurassic epicontinental carbonates and mudstones from England and Wales: chemostratigraphic signals and the early Toarcian anoxic event. Sedimentology 44, 687–706.
Jenkyns, H.C., Jones, C.E., Gröcke, D.R., Hesselbo, S.P., Parkinson, D.N., 2002. Chemostratigraphy of the Jurassic system: applications, limitations and implications for palaeoceanography. J. Geol. Soc. Lond. 159, 351–378.
Jiménez, A.P., Jiménez de Cisneros, C., Rivas, P., Vera, J.A., 1996. The early Toarcian anoxic event in the westernmost Tethys (Subbetic): Paleogeographic and paleobiogeographic significance. J. Geol. 104, 399–416.
Jones, C.E., Jenkyns, H.C., Hesselbo, S.P., 1994. Strontium isotopes in Early Jurassic seawater. Geochim. Cosmochim. Acta 58, 1285–1301.
Jourdan, F., Féraud, G., Bertrand, H., Watkeys, M.K., Renne, P.R., 2008. The $^{40}Ar/^{39}Ar$ ages of the sill complex of the Karoo large igneous province: implications for the Pliensbachian–Toarcian climate change. Geochem. Geophys. Geosyst. 9, Q06009. http://dx.doi.org/10.1029/2008GC001994.
Korte, Ch., Hesselbo, S.P., Ullmann, C.V., Dietl, G., Ruhl, M., Schweigert, G., Thibault, N., 2015. Jurassic climate mode governed by ocean gateway. Nat. Commun. 6, 10015. http://dx.doi.org/10.1038/ncomms10015.
Küspert, W., 1982. Environmental changes during oil shale deposition as deduced from stable isotope ratios. In: Einsele, G., Seilacher, A. (Eds.), Cycles and events in Stratigraphy. Springer, Berlin, pp. 482–501.
Li, Q., McArthur, J.M., Atkinson, T.C., 2012. Lower Jurassic belemnites as indicators of palaeo-temperature. Palaeogeogr. Palaeoclimatol. Palaeoecol. 315–316, 38–45.
Little, C.T.S., Benton, M.J., 1995. Early Jurassic mass extinction–a global long term event. Geology 23, 495–498.
Littler, K., Hesselbo, S.P., Jenkyns, H.C., 2010. A carbon-isotope perturbation at the Plienbachian–Toarcian boundary: evidence from the Lias Group, NE England. Geol. Mag. 147, 181–192.
Marshall, J.D., 1992. Climatic and oceanographic isotopic signals from the carbonate rock record and their interpretation. Geol. Mag. 129, 134–160.
McArthur, J.M., 1994. Recent trends in strontium isotope stratigraphy. Terra Nova 6, 331–358.
McArthur, J.M., Donovan, D.T., Thirlwall, M.F., Fouke, B.W., Mattey, D., 2000. Strontium isotope profile of the early Toarcian (Jurassic) oceanic anoxic event, the duration of ammonite biozones, and belemnite palaeotemperatures. Earth Planet. Sci. Lett. 179, 269–285.
McArthur, J.M., Doyle, P., Leng, M.J., Reeves, K., Williams, C.T., Garcia-Sanchez, R., Howarth, R.J., 2007. Testing palaeo-environmental proxies in Jurassic belemnites: Mg/Ca, Sr/Ca, Na/Ca, $\delta^{18}O$ and $\delta^{13}C$. Palaeogeogr. Palaeoclimatol. Palaeoecol. 252, 464–480.
McCrea, J.M., 1950. On the isotopic chemistry of carbonates and a paleotemperature scale. J. Chem. Phys. 18 (6), 849–857.
McElwain, J.C., Wade-Murphy, J., Hesselbo, S.P., 2005. Changes in carbon dioxide during an oceanic anoxic event linked to intrusion into Gondwana coals. Nature 435, 479–482.
Metodiev, L., Koleva-Rekalova, E., 2008. Stable isotope records ($\delta^{18}O$ and $\delta^{13}C$) of Lower-Middle Jurassic belemnites from the western Balkan mountains (Bulgaria): Palaeoenvironmental application. Appl. Geochem. 23, 2845–2856.
Montero-Serrano, J.-C., Föllmi, K.B., Adatte, T., Spangenberg, J.E., Tribovillard, N., Fantasia, A., Suan, G., 2015. Continental weathering and redox conditions during the early Toarcian oceanic anoxic event in the northwestern Tethys: insight from the Posidonia shale section in the Siwss Jura Mountains. Palaeogeogr. Palaeoclimatol. Palaeoecol. 429, 83–99.
Nolan, H., 1895. Sur le Jurassique et le Crétacé des iles Baleares. C. R. Acad. Sci. Paris 117, 821–823.
Nunn, E.V., Price, G.D., 2010. Late Jurassic (Kimmeridgian–Tithonian) stable isotopes ($\delta^{18}O$, $\delta^{13}C$) and Mg/Ca ratios: new palaeoclimate data from Helmsdale, northeast Scotland. Palaeogeogr. Palaeoclimatol. Palaeoecol. 292, 325–335.
Page, K.N., 2003. The Lower Jurassic of Europe: its subdivisión and correlation. Geol. Survey Denmark Greenland Bull. 1, 23–59.
Pálfy, J., Smith, P.L., 2000. Synchrony between Early Jurassic extinction, oceanic anoxic event, and the Karoo-Ferrar flood basalt volcanism. Geology 28, 747–750.
Pittet, B., Suan, G., Lenoir, F., Duarte, L.V., Mattioli, E., 2014. Carbon isotope evidence for sedimentary discontinuities in the lower Toarcian of the Lusitanian Basin (Portugal): sea level change at the onset of the oceanic anoxic event. Palaeogeogr. Palaeoclimatol. Palaeoecol. 303, 1–14.
Podlaha, O.G., Mutterlose, J., Veizer, J., 1998. Preservation of $\delta^{18}O$ and $\delta^{13}C$ in belemnite rostra from the Jurassic/early Cretaceous successions. Am. J. Sci. 298, 324–347.
Prescott, D.M., 1988. The geochemistry and palaeoenvironmental significance of iron pisoliths and ferromanganese crusts from the Jurassic of Mallorca, Spain. Eclogae Geol. Helv. 81, 387–414.
Price, G.D., 1999. The evidence and implications of polar ice during the Mesozoic. Earth Sci. Rev. 48, 183–210.
Price, G.D., Williamson, T., Henderson, R.A., Gagan, M.K., 2012. Berremian–Cenomanian palaeotemperatures for Australian seas based on new oxygen-isotope data from belemnite rostra. Palaeogeogr. Palaeoclimatol. Palaeoecol. 358-360, 27–39.
Price, G.D., Baker, S.J., Van de Valde, J., Clémence, M.-E., 2016. High-resolution carbon cycle and seawater temperature evolution during the Early Jurassic (Sinemurian–early Pliensbachian). Geochem. Geophys. Geosyst. 17, 3917–3928. http://dx.doi.org/10.1002/2016GC006541.
Quesada, S., Robles, S., Rosales, I., 2005. Depositional architecture and transgressive–regressive cycles within Liassic backstepping carbonate ramps in the Basque–Cantabrian Basin, northern Spain. J. Geol. Soc. Lond. 162, 531–548.
Röhl, H.-J., Schmid-Röhl, A., Oschmann, W., Frimmel, A., Schwark, L., 2001. The Posidonia shale (lower Toarcian) of SW-Germany: an oxygen-depleted ecosystem controlled by sea level and palaeoclimate. Palaeogeogr. Palaeoclimatol. Palaeoecol. 165, 27–52.
Rosales, I., Quesada, S., Robles, S., 2001. Primary and diagenetic isotopic signals in fossils and hemipelagic carbonates: the Lower Jurassic of northern Spain. Sedimentology 48, 1149–1169.
Rosales, I., Quesada, S., Robles, S., 2004a. Paleotemperature variations of Early Jurassic seawater recorded in geochemical trends of belemnites from the Basque–Cantabrian Basin, northern Spain. Palaeogeogr. Palaeoclimatol. Palaeoecol. 203, 253–275.
Rosales, I., Robles, S., Quesada, S., 2004b. Elemental and oxygen isotope composition of Early Jurassic belemnites: salinity vs. temperature signals. J. Sediment. Res. 74, 343–355.
Rosales, I., Quesada, S., Robles, S., 2006. Geochemical arguments for identifying second-order sea-level changes in hemipelagic carbonate ramp deposits. Terra Nova 18, 233–240.
Ruebsam, W., Münzberger, P., Schwark, L., 2014. Chronology of the early Toarcian environmental crisis in the Lorraine sub-basin (NE Paris Basin). Earth Planet. Sci. Lett. 404, 273–282.
Sabatino, N., Vlahović, I., Jenkyns, H.C., Scopelliti, G., Neri, R., Prtoljan, B., Velić, I., 2013. Carbon-isotope record and palaeoenvironmental changes during the early Toarcian oceanic anoxic event in shallow-marine carbonates of the Adriatic carbonate platform in Croatia. Geol. Mag. 150, 1085–1102. http://dx.doi.org/10.1017/S0016756813000083.
Sælen, G., Doyle, P., Talbot, M.R., 1996. Stable-isotope analyses of belemnite rostra from the Whitby mudstone Fm, England: surface water conditions during deposition of a marine black shale. PALAIOS 11, 97–117.
Suan, G., Mattioli, E., Pittet, B., Mailliot, S., Lécuyer, Ch., 2008. Evidence for major environmental perturbation prior to and during the Toarcian (Early Jurassic) oceanic

anoxic event from the Lusitanian Basin, Portugal. Paleoceanography 23, PA1202. http://dx.doi.org/10.1029/2007PA001459.
Suan, G., Mattioli, E., Pittet, B., Lécuyer, Ch., Suchéras-Marx, B., Duarte, L.V., Philippe, M., Reggiani, L., Martineau, F., 2010. Secular environmental precursors to early Toarcian (Jurassic) extreme climate changes. Earth Planet. Sci. Lett. 290, 448–458.
Suan, G., Nikitenko, B.L., Rogov, M.A., Baudin, F., Spangenberg, J.E., Knyazev, V.G., Glinskikh, L.A., Goryacheva, A.A., Adatte, T., Riding, J.B., Föllmi, K.B., Pittet, B., Mattioli, E., Lécuyer, Ch., 2011. Polar record of Early Jurassic massive carbon injection. Earth Planet. Sci. Lett. 312, 102–113.
Swart, P.K., Eberli, G.P., 2005. The nature of the $\delta^{13}C$ of periplatform sediments: implications for stratigraphy and global carbon cycle. Sediment. Geol. 175, 115–129.
Ullmann, C.V., Thibault, N., Ruhl, M., Hesselbo, S.P., Korte, Ch., 2014. Effect of a Jurassic oceanic anoxic event on belemnite ecology and evolution. PNAS 111, 10073–10076.
Ullmann, C.V., Frei, R., Korte, C., Hesselbo, S.P., 2015. Chemical and isotopic architecture of the belemnite rostrum. Geochim. Cosmochim. Acta 159, 231–243.
Val, J., Bádenas, B., Aurell, M., Rosales, I., 2017. Cyclostratigraphy and chemostratigraphy of a bioclastic storm-dominated carbonate ramp (late Pliensbachian, Iberian Basin). Sediment. Geol. 355, 93–113.
van de Schootbrugge, B., McArthur, J.M., Bailey, T.R., Rosenthal, Y., Wright, J.D., Miller, K.G., 2005a. Toarcian oceanic anoxic event: an assessment of global causes using belemnite C isotopes records. Paleoceanography 20, PA3008. http://dx.doi.org/10.1029/2004PA001102.
van de Schootbrugge, B., Bailey, T.R., Rosenthal, Y., Katz, E.M., Wright, J.D., Miller, K.G., Feist-Burkhardt, S., Falkowski, P.G., 2005b. Early Jurassic climate change and the radiation of organic-walled phytoplankton in the Tethys Ocean. Paleobiology 31, 73–97.
Wierzbowski, H., 2004. Carbon and oxygen isotope composition of Oxfordian–early Kimmeridgian belemnite rostra: palaeoenvironmental implications for Late Jurassic seas. Palaeogeogr. Palaeoclimatol. Palaeoecol. 203, 153–168.
Wierzbowski, H., Joachimski, M.M., 2007. Reconstruction of late Bajocian–Bathonian marine palaeoenvironments using carbon and isotope ratios of calcareous fossils from the polish Jura chain (central Poland). Palaeogeogr. Palaeoclimatol. Palaeoecol. 254, 523–540.
Wignall, P.B., Newton, R.J., Little, C.T.S., 2005. The timing of paleoenvironmental change and cause-effect relationships during the Early Jurassic mass extinction in Europe. Am. J. Sci. 305, 1014–1032.